Summer 2021

Neuronal Migration in Developmental Hyperserotonmia: Assessment of Vesicular Glutamate in the Raphe Nuclei

Trey M. Shupp
Missouri State University, Shupp3197@live.missouristate.edu

NEURONAL MIGRATION IN DEVELOPMENTAL HYPERSEROTNEMIA: ASSESSMENT OF VESICULAR GLUTAMATE IN THE RAPHE NUCLEI

A Master's Thesis

Presented to

The Graduate College of

Missouri State University

In Partial Fulfillment

Of the Requirements for the Degree

Master of Science, Cell and Molecular Biology

By

Trey Marlin Shupp

July 2021

NEURONAL MIGRATION IN DEVELOPMENTAL HYPERSEROTNMIA:

ASSESSMENT OF VESICULAR GLUTAMATE IN THE RAPHE NUCLEI

Biomedical Sciences

Missouri State University, July 2021

Master of Science

Trey Marlin Shupp

ABSTRACT

The neurotransmitter serotonin is involved in the early development of the central nervous system and the organization of neurons throughout the cerebral cortex and cerebellum. It is proposed that serotonin indirectly interacts with cells in the marginal zone of the cerebral cortex known as Cajal-Retizus (CR) cells. These cells secrete the extracellular matrix protein reelin, which is known for its role in neuronal organization and migration during early neural development. It has been observed that low levels of serotonin are associated with similarly low levels of reelin during development and have been reported to result in disorganization of neurons in the cortical layers. Similarly, neuronal disorganization of the cortex has also been reported in response to increased levels of developmental serotonin which in-turn can lower serotonin levels in the developed brain due to activation of an autoregulatory negative feedback mechanisms. For reelin to be secreted by the CR cells, the neurotransmitter γ-aminobutyric acid (GABA) needs to be available to interact with the $GABA_A$ receptor on the CR cells themselves. However, GABA is associated with the Glutamate/GABA excitatory and inhibitory feedback system where high levels of glutamate will stimulate release of GABA and vice versa. These neurotransmitters regulate the activity of many key processes such as overall excitation of the brain and is proposed to have a role in the organization and migration of neurons during development. It is known that serotonin is the early regulator of glutamate release in the cell which in turn activates the release of GABA. However, it is thought that in conditions where excess serotonin is released during development (hyperserotonemia) that serotonin will inhibit glutamate release instead of activation. This study proposes to investigate the methodological processes necessary to analyze the correlation of excess developmental serotonin on the neurotransmitter glutamate. This was conducted by identifying the dorsal raphe nuclei via cresyl violet staining on control Sprague-Dawley rat brain tissues while investigation of glutamate release levels in development was performed via immunohistochemical labeling of vesicular glutamate transporters in the dorsal raphe nuclei.

KEYWORDS: Autsim Spectrum Disorder (ASD), developmental hyperserotonemia (DHS), Cajal-Retizus cells, reelin, serotonin, cortical development

NEURONAL MIGRATION IN DEVELOPMENTAL HYPERSEROTNMIA:

ASSESSMENT OF VESICULAR GLUTAMATE IN THE RAPHE NUCLEI

By

Trey Marlin Shupp

A Master's Thesis
Submitted to the Graduate College
Of Missouri State University
In Partial Fulfillment of the Requirements
For the Degree of Master of Science, Cell and Molecular Biology

July 2021

Approved:

Lyon H. Hough, Ph.D., Thesis Committee Chair

Scott D. Zimmerman, Ph.D., Committee Member

Henry P. Tsai, Ph.D., Committee Member

Julie Masterson, Ph.D., Dean of the Graduate College

TABLE OF CONTENTS

LIST OF TABLES

LIST OF FIGURES

LITERATURE REVIEW

Autism Spectrum Disorder

Autism Spectrum Disorder (ASD) is an increasingly prevalent neurodevelopmental disorder characterized by three core deficits: impaired communication, impaired social interactions, and restricted, repetitive and stereotyped patterns of behavior and/or interests (Faras et al., 2010; Maenner, 2020). However, not all presentations of ASD are the same, with severity, range, and involvement of symptoms varying across individuals (Faras et al., 2010). Additionally, the exact cause of ASD is still unknown as researchers work to further elucidate this complex multifactorial disorder. As such, there has been a growing interest in the relationship of ASD to neurological comorbidities, potential treatments, and the underlying neural circuitry involved in the disorder (Jeste, 2011).

Since the year 2000, the Center for Disease Control and Prevention's (CDC) Autism and Developmental Disabilities Monitoring (ADDM) Network has reported the prevalence of developmental disabilities with attention to Autism Spectrum Disorder (ASD). The CDC and the Human Resources and Services Administration (HRSA) conducted a study on how often developmental disabilities were diagnosed in the United States. It was found that between the years 2009-2011 that 16.2% of children aged 3-17 were diagnosed with some sort of disability. Yet, when compared to 2015-2017, the numbers have increased to 17.8% of children (Zablotsky et al., 2019). Of the developmental disabilities, ASD has been increasingly prevalent as it was previously estimated that 1 in 150 children at the age of 8 were diagnosed with ASD in between the years 2000-2002. However, by 2016 the number of children diagnosed with ASD climbed to 1 in 54 (Baio et al., 2018; Maenner, 2020). An increase that has not been fully explained due to

increased awareness or diagnosis. Instead, researchers agree that there are likely strong environmental and genetic factors at play to explain the dramatic increases in ASD prevalence. ASD goes beyond all social, economic, and racial backgrounds and is known to affect families from all walks of life. Yet, it has been observed that ASD displays a bias towards the male sex with 1 female diagnosed for every 4 males (Baio et al., 2018; Maenner, 2020).

Diagnosis of ASD is restricted to guidelines set by the current Diagnostic and Statistical Manual of Mental Disorders, Fifth Edition (DSM-5). Although manifestations of ASD can be found in a wide spectrum, five conditions must be met in order to be considered ASD. However, these do not include all comorbidities that have been observed and associated with ASD. The first two conditions consist of symptoms being present in early development and may be experienced throughout their lives. It is common for individuals to mask their symptoms later in life but is not always the case. Additionally, symptoms must clinically impair social, occupational, and functional elements of life in order to be diagnosed as ASD in addition to the criteria described in the DSM-5 (APA, 2013).

The remaining criteria involve three levels of deficit in social communication and interaction. Although the severity of impairment can vary, all three criteria are required for ASD diagnosis. The first area includes deficits in social-emotional reciprocity. This is presented by failure in normal interactions where a back-and-forth interaction is difficult. It can also present itself in reduced sharing of emotions and abnormal social approaches such as failure to initiate communication. The second deficit is in nonverbal communication. When deficits in nonverbal communication are present, individuals with ASD may avoid eye contact, conduct abnormal body language, and have little understanding of gestures. Lastly, deficits in social communication which involve developing and maintaining relationships are commonly observed

in ASD. Those with ASD have difficulties developing and maintaining relationships due to a lack of social understanding which can range from difficulty adjusting to new people to a complete lack of interest in peers. As a result, difficulty in social context can become a burden to those diagnosed with ASD (APA, 2013).

Repetitive and restrictive patterns of behavior and interests are closely associated with the core characteristics of ASD. Repetitive and restrictive patterns can present in various degrees of severity. In order to receive an ASD diagnosis, two of four repetitive/restrictive behaviors must be presented and observed (APA, 2013). The first pattern presents itself as stereotyped or repetitive motor movements, object use, and/or speech. Examples of these behaviors include repetitive motor manners such as flapping of hands, flicking or twisting their fingers, or rocking back and forth (Kim and Lord, 2010). Individuals can also present more verbal patterns of behavior where those with ASD talk with idiosyncratic phrases. This can appear as overly specific details used in conversation where irrelevant content is brought up with extensive digressions (Rouhizadeh et al., 2015). Another presentation of repetitive patterns of behaviors includes strict insistence on sameness and being inflexible to routines. Change to normal routines can cause extreme distress in individuals with ASD and causes difficulty transitioning from one task to another. This can manifest in simple changes to schedules, foods, conversation topics, and traveling routes. Additionally, another common feature of ASD is highly restrictive fixations on objects and interests that would otherwise be abnormal. Children with ASD will often examine small parts of objects such as wheels on toy cars extensively with little yield from distraction (Jossin et al., 2003; Chameau et al., 2009; Marín-Padilla, 2015; Buchsbaum and Cappello, 2019; Kim and Lord, 2010). The last presentation of restrictive and repetitive behaviors includes a hyper- or hypo-reactivity to sensory input or an unusual interest in sensory aspects of the

environment. These individuals will have an abnormal level of attraction to sensory aspects of life but also contain unusual sensorimotor processing. Common observations include being unable to differentiate between pain/temperature, extreme sensitivity to sound or light, and excessive smelling and touching of objects (APA, 2013).

As a developmental disorder, increased focus on neurological development has since occurred with multiple neuronal structures being implicated in ASD. Many symptoms listed in the DSM-5 such as abnormal motor manners, defects in verbal/non-verbal communication, and unusual sensorimotor processing have been linked to changes within neurological morphology. One possible cause to this could be investigated through study in the serotonergic pathway in early development. It has been reported that the most common biomarker for ASD has been elevated whole blood serotonin levels also known as hyperserotonemia. These elevated levels were found in more than 25% of affected children and points to a possible root for ASD. (Whitaker-Azmitia, 2001; McNamara et al., 2008; Hough and Segal, 2016; Aaron et al., 2019). Models have been proposed in order to further the understanding of ASD with one such model known as the developmental hyperserotonemia (DHS) model (Hadjikhani, 2010).

Developmental Hyperserotonemia Model

The developmental hyperserotonemia model was first proposed through the observation that high levels of whole-blood serotonin were found in many autistic patients (Schain and Freedman, 1961). Over the course of 30 years, multiple studies investigating the correlation of serotonin and ASD has provided evidence of hyperserotonemia in approximately one-third of all autistic patients (Lam et al., 2006; Cook et al., 1993; Anderson et al., 1990; McBride et al., 1998). It is this factor that makes hyperserotonemia appealing as a model for studying ASD and

the contributing causes of neurological disorders (Shemer et al., 1988; Shemer et al., 1991; Whitaker-Azmitia, 2004; Hadjikhani, 2010).

In 1987, Shemer et al. reported increasing evidence in tissue models that neuronal outgrowth would be altered during the presence of agonists of serotonin. Not only were these agonists altering maturation, but one such agonist known as 5-methoxytryptamine (5-MT) was found endogenously in rodent brains and mimics the effects of serotonin (Shemer et al., 1988). Using 5-MT, experiments were conducted to understand the effects of this agonist on both serotonin reuptake and behavior when neonatal rats were exposed to high levels of agonist. It was reported that 5-MT reduces the uptake of serotonin during birth and indirectly inhibits neuronal outgrowth and maturation of serotonergic neurons throughout the cerebral cortex. Therefore, by introducing 5-MT or other serotonin agonists during development, it could possibly influence early development and neuronal organization within the cerebral cortex (Shemer et al., 1991; Whitaker-Azmitia, 2004). Using the proposed hypothesis that high levels of serotonin in the blood may lead to some behavioral and cellular changes, McNamara et al. (2008) further investigated the developmental hyperserotonemia model and its potential role in neurological disorders such as ASD (McNamara et al., 2008).

In order to assess the validity of the DHS model for ASD, multiple translational behavioral studies of these rats were conducted to compare with behavioral deficits reported in the ASD population. In these investigations, timed-pregnant dams were exposed to the serotonin agonist 5-MT beginning on gestational day 12 to mimic high levels of developmental serotonin. It was anticipated that if the rat model developed cardinal features of autism such as deficits in social communication, then it could also be used as a model to study ASD. (McNamara et al., 2008). Subsequent rat pups were similarly treated with exogenous 5-MT until postnatal day 20.

Behavioral testing was conducted on the rat pups to determine the underlying effects of exposure to high levels of developmental serotonin.

The immediate response to the exposure to 5-MT was infantile seizures. In one study, 48 out of 41 pups experienced severe seizure-like behaviors during post-natal day 8. However, pups treated with saline contained no seizure activity. With ASD sharing 25% comorbidity with epilepsy, these results indicate that increased amount of agonist could be affecting neuropeptides associated with seizure activity. Along with this, the serotonergic 5-HT_{1A} receptor is known to reduce seizure activity that is caused by increased kainic acid. Within DHS model of rats, the 5-HT_{1A} receptor is inhibited within the temporal lobe at the epileptic foci. Thus, it is possible that high levels of serotonin induced seizure like behavior. Additionally, rats that were exposed to 5-MT exhibited social deficits where pups strayed away from their litter more often than those that were exposed to saline, exhibited increased repetitive behaviors including gnawing and exposure to painful stimuli, and spent a decreased amount of time engaged in olfactory interactions with other rat pups. Each of these behaviors can be linked with observed behaviors seen in ASD patients whom experience loss of social interaction, social communication, and repeated/repetitive patterns of behaviors. Additionally, hyperserotonemia is considered the most common biomarker within patients that have ASD and using a developmental hyperserotonemia (DHS) model of rats, it was observed that high levels of 5-HT show behavioral and morphological changes that is similar to those observed in ASD in humans (Whitaker-Azmitia, 2001; McNamara et al., 2008; Hough and Segal, 2016; Aaron et al., 2019). Thus, serotonin is thought to be a key factor in ASD and is associated with early neuronal development and, through disruption, can alter the development of the serotonergic neurons in the cortex.

Serotonergic System

5- hydroxytryptamine (5-HT), more commonly known as serotonin, is a neurotransmitter involved in many areas of neuronal activity (Brummelte et al., 2017; Shehabeldin et al., 2018). 5-HT plays a key regulatory role within the body through processes such as appetite, motor functions, and both cognitive and autonomic behavior including the regulation of energy, GI function, and cardiovascular and pulmonary physiology (Berger et al., 2009; Brummelte et al., 2017; Shehabeldin et al., 2018). In addition to its role as a neurotransmitter, 5-HT has been shown to act as a developmental neuronal growth factor through involvement in processes such as cell proliferation, migration, differentiation, neurogenesis, synaptogenesis, and facilitating dendritic elaboration. (Whitaker-Azmitia, 2001; Shehabeldin et al., 2018). It is during these early developmental stages that the 5-HT system is hypothesized to play a central role in the development of the central nervous system (Brummelte et al., 2017; Shehabeldin et al., 2018). Conversely, disruption of the serotonergic system and its developmental signaling pathway has been associated with many developmental neurological disorders such as autism and schizophrenia (Berger et al., 2009; Brummelte et al., 2017; Shehabeldin et al., 2018).

During the early stages of neuronal development, the serotonergic neurons are expressed at specific locations along the neural tube, the embryonic precursor to the central nervous system. It has been found in rats that beginning on gestational day 10, the majority of the serotonergic neurons are expressed at the ventral midline of the neural tube on a structure known as the floor plate. Yet, they are not visually evident until gestational week five (Placzek et al., 1993; Brummelte et al., 2017; Shehabeldin et al., 2018). By the 15th week, the serotonergic neurons are found in distinct arrangements in the raphe nuclei (Hornung, 2003; Brummelte et al.,

2017). These raphe nuclei are located along the brainstem where serotonergic neurons are contained to release serotonin and create synaptic connections (Figure 1).

The clusters of cells (B1-B9) that contain serotonergic neurons are what is known as the raphe nuclei system and are organized by the distribution in the brainstem (Figure 1,2). Although restricted to the midline, these clusters give rise to the serotonergic projections that extend to nearly all areas of the CNS (Shehabeldin et al., 2018; Hornung, 2010). In humans, the raphe nuclei system is arranged along the longitudinal axis into two distinct groups defined as the rostral and caudal raphe nuclei (Hornung, 2003; Hornung, 2010; Brummelte et al., 2017; Shehabeldin et al., 2018). Rat models used in research for neurological disorders such as ASD are often used visualize the location of individual groups along the raphe nuclei. For the remainder of this review section, rat models will be used for context (Figure 2). Beginning with the caudal group, the nuclei can be further subdivided into three individual subgroups of (B1 – B3) seen in a rat model (Figure 2). These groups extend from the caudal metencephalon to the junction of the brainstem and spinal cord (Hornung, 2003; Hornung, 2010). The raphe pallidus nucleus (RPa, B1) is the smallest of the raphe nuclei that contains long, slender neurons that have very few dendritic processes. However, the raphe pallidus has been shown to play roles the mediation of tachycardia and fever induction after development (Zaretsky et al., 2003). The raphe obscurus nucleus (Rob, B2) extends rostro-caudally from the facial nucleus and contains small to medium sized serotonergic neurons located along the midline (Figure 2).

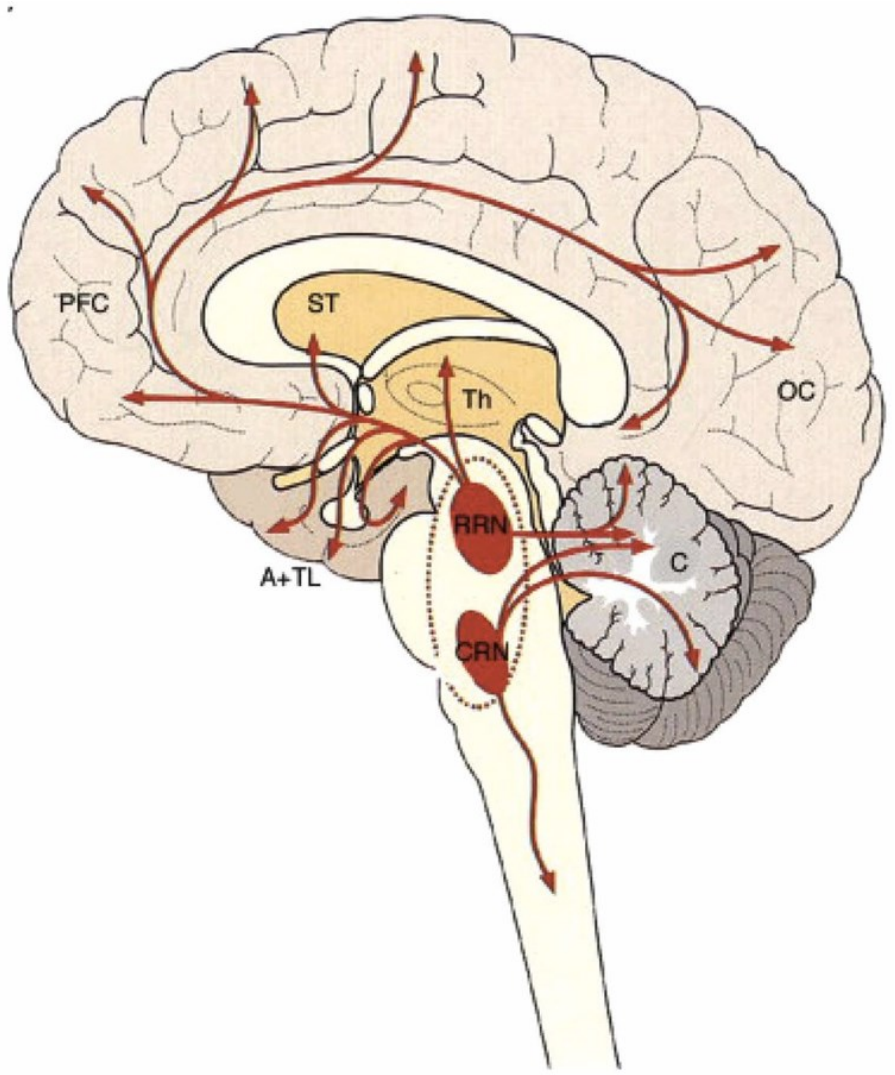

Figure 1 | Locations of the Raphe Nuclei Along the Brainstem. An adult human brain illustrates the location of the rostral raphe nuclei (RRN) and the caudal raphe nuclei (CRN) in relation to the cerebellum I, the brainstem, and the prefrontal cortex (PFC) (Figure taken from Evers et al., 2010).

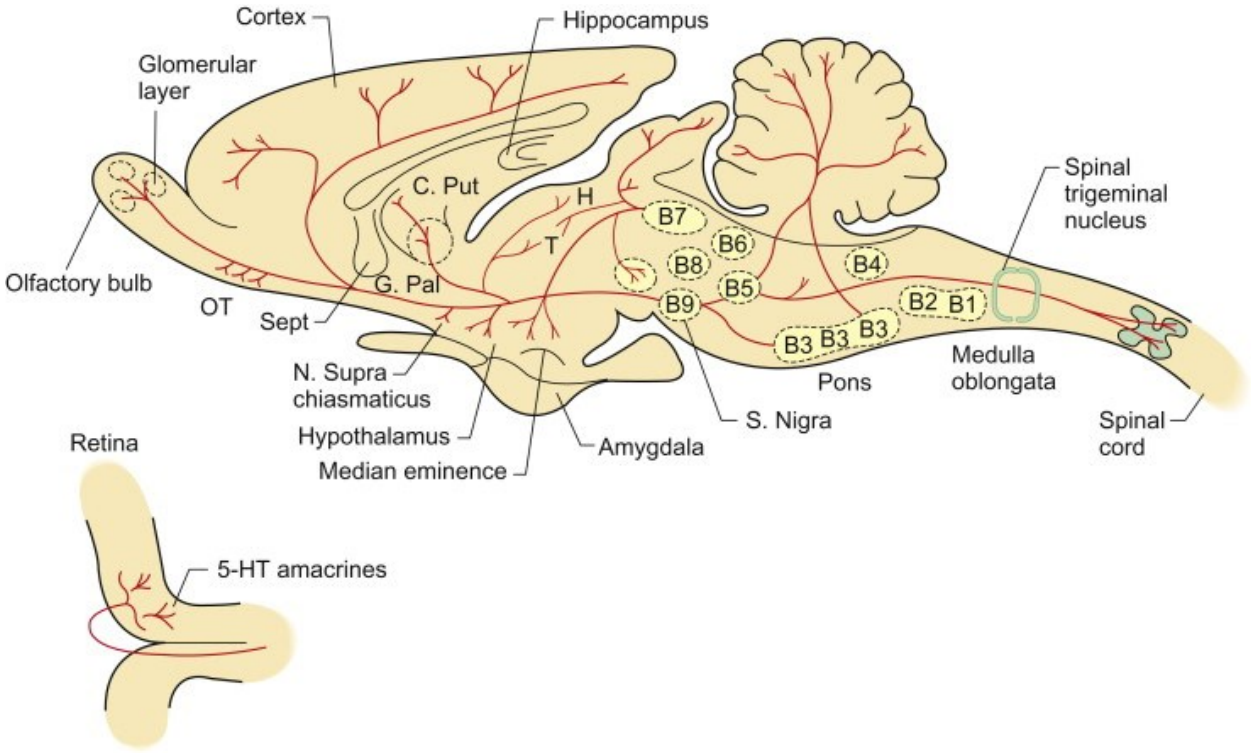

Figure 2 | Schematic of a sagittal section of the central nervous system within a rat. The raphe system divided into clusters of serotonergic neurons. The caudal raphe nuclei: raphe pallidus nucleus, B1; raphe obscurus nucleus, B2; raphe magnus nucleus, B3. The rostral raphe nuclei: caudal linear nucleus, B8; dorsal raphe nuclei, B6-B7; median raphe nucleus, B5. (Figure taken from: George J. Siegel's, Basic Neurochemistry, 1999

The last group in the caudal region is the raphe magnus nucleus (RMg, B3) which contains serotonergic neurons that extend laterally with the lateral reticular formation at the junction between the medulla and pons (Hornung, 2003; Hornung, 2010). The rostral group contains subdivisions that extend from the caudal mesencephalon to the mid pons and include the caudal linear nucleus, the dorsal raphe nucleus, and the median raphe nucleus (Hornung, 2003; Hornung, 2010). The caudal linear nucleus (Cli, B8-B9) contains serotonergic neurons with elongated dendritic fibers that are in a rostro-caudal direction which are parallel to the midline plane. Statistically, there are less neurons located in this nucleus in comparisons to the dorsal raphe nucleus which the caudal linear nucleus merges into at the most rostral portion. The dorsal raphe nucleus (DR, B6-B7) is the largest group of serotonergic neurons and accounts for one third of the population in the brain. These neurons will extend throughout the central nervous system including the forebrain, the caudate-putamen and parieto-temporal cortex, thalamus, hypothalamus, and the midbrain (Azmitia and Segal, 1978). Lastly, the median raphe nucleus (MnR, B5) are made of serotonergic neurons extending elongated projections from the midline paralaterally (Figure 2) (Hornung, 2003; Hornung, 2010; Shehabeldin et al., 2018).

All of the raphe nuclei are involved in the release of the serotonergic neurotransmitter throughout the entirety of the central nervous system (Hornung, 2003; Hornung, 2010). The rostral serotonergic system will provide axonal projections to the midbrain, forebrain, and the cerebellum, whereas the caudal serotonergic system will send projections down the brainstem to the spinal cord where it will provide parallel projections to the dorsal, intermediate, and ventral columns of the spinal cord. (Hornung, 2003; Hornung, 2010; Shehabeldin et al., 2018). However, axonal outgrowth out of the raphe nuclei is not simple. Migration involves a complex signaling pathway that when disrupted could change the morphology of the neurons and their projections

in the CNS. Due to this, it is important to understand the organization of the cerebral cortex and the areas in which axons project during development.

Cerebral Cortex

Within the human brain there are three divisions of the cerebral cortex; the neocortex, paleocortex, and archicortex (Young et al., 2012). The paleocortex and archicortex make up the allocortex which is located in the medial temporal lobes of the brain (Swenson, 2006). The allocortex are phylogenetically older areas of the cortex and are involved with the olfactory system and the hippocampus along with many primary bodily functions such as vision and sensation (Swenson, 2006; Young et al., 2012). The neocortex makes up the majority of the cerebral cortex and contains six layers that include up to 14 billion neurons which are involved in higher cognitive behavior and function in humans (Swenson, 2006; Young et al., 2012). Each of these layers is numbered using the Roman numeral system from superficial layer (I) to the deepest (VI). Further, these layers can be separated into three groups; the supergranular layers (I-III), the inner granular layer (IV), and the infragranular layers (V-VI) (Swenson, 2006). The infragranular layer is primarily involved in the motor cortical areas with layer V producing cortical efferent projections to the brain stem and spinal cord whereas layer VI projects to the thalamus. The inner granular layer (IV) will receive sensory input and is the primary sensory cortex in the brain (Swenson, 2006). Lastly, the supraganular layers (I-III) are the primary intercortical connections to allow communication between the different hemispheres of the brain but also within the same hemisphere (Figure 3,4).

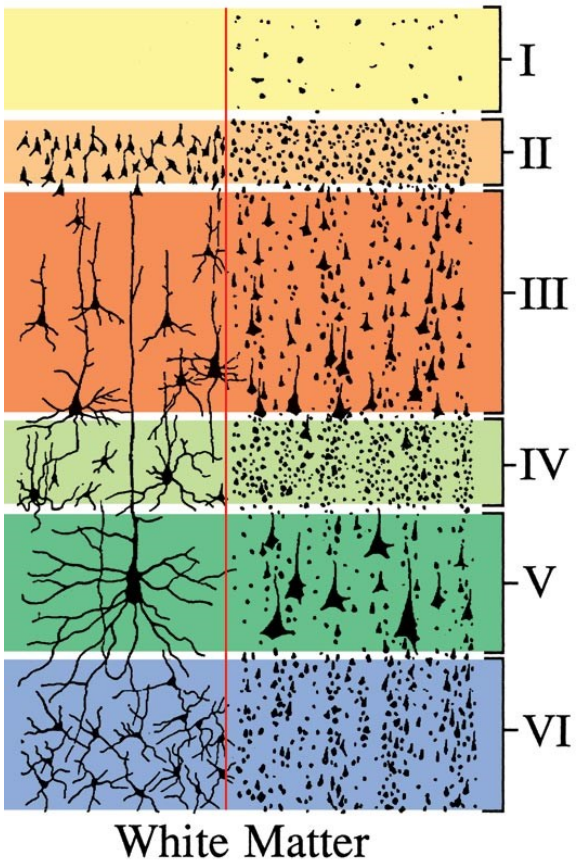

Figure 3 | Organization of the Neocortex. The neocortex is made up of six distinct layers; Molecular Layer (I) External Granular Layer (II), External Pyramidal Layer (III), Internal Granular Layer (IV), Internal Pyramidal Layer (V), Multiform Layer (VI). Three groups can be formed from these layers; Supragranular layer (I-III), Inner Granular Layer (IV), and the Infragranular Layer (V-VI). (Ranson and Clark, 1959).

All of the organization in the neocortex is completed through the migration of neurons both tangentially and radially during the first stages of embryonic development (Gil et al., 2014). The first stage of the development of the neocortex involves the formation of the preplate which is made of a superficial plexus of nerve fibers and post-migratory cells such as the Cajal-Retizus cells, interneurons, and subplate neurons (Gil et al., 2014). The preplate contains post-migratory cells that exit the ventricular zone of the cortex and move radially with the radial glial cells guiding them. Lastly, the post-migratory cells will split at the pial surface into two distinct layers; the molecular zone (MZ) and the subplate (Gil et al., 2014). The MZ will be located above the subplate and contain Cajal-Retizus (CR) cells and then establish the cortical plate (layers II-VI).

Cajal-Retzius Cells and Serotonergic Connections

Within the MZ, Cajal-Retzius cells are among the first developed in the cortex and their primary role early in development is to synthesize and secrete the extracellular matrix glycoprotein called reelin (Chameau et al., 2009). The protein reelin orchestrates the migration of many neuroblasts through the use of radial glial cells that act as guides to the neurons (Marín-Padilla, 2015). These cells are responsible for the correct organization of the lamina of the neocortex. It is during the early migration of the serotonin-containing axonal projections that Cajal-Retzius cells will establish synaptic connections within the neocortex (Shehabeldin et al., 2018). In order for this to occur, serotonergic neurons will migrate from the ventricular zone along the midline in order to reach the CP or MZ (Figure 4). From here, the serotonergic projections will continue migrating postnatally extending to their final locations outside of the raphe nuclei.

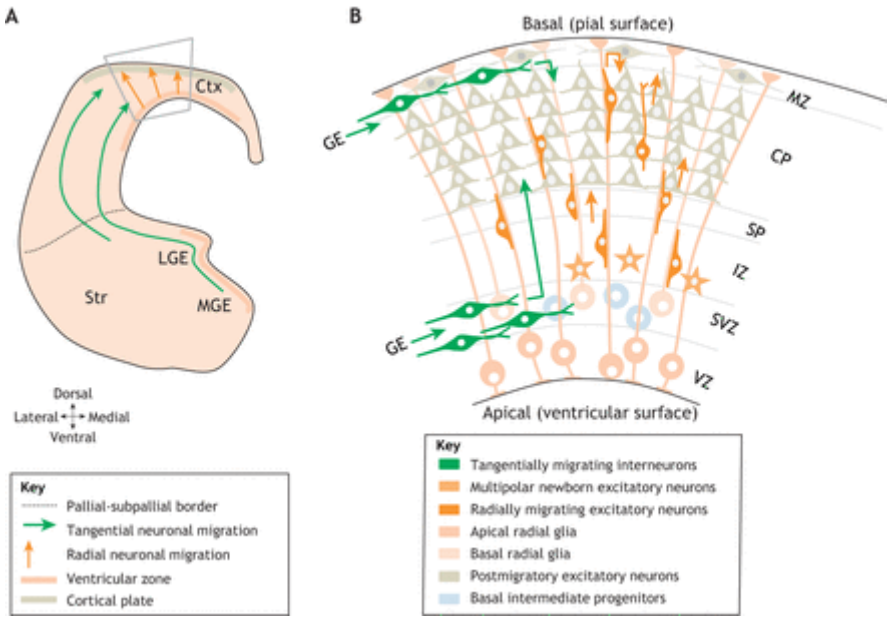

Figure 4 | Neuronal Migration From the Ventricular Zone. Neurons will begin migration from the ventricular zone (VZ) and move in a radial direction to the marginal zone (MZ). It is at the cortical plate and marginal zone that synaptic connections will be made with cells such as Cajal-Retizus cells (Buchsbaum, 2019).

It is in the caudal serotonergic system that the serotonergic projections are thought to be involved with mood changes, emotional behavior, and select conditions that influence the levels of serotonin in the blood such as hyposerotonemia (low levels of serotonin) and hyperserotonemia (high levels of serotonin). After migration, the axonal arborizations will establish synaptic connection with the forebrain, cerebellum, and midbrain. The projections that extend to the neocortex will create those synaptic connections with the Cajal-Retzius cells that will then have a leading role in serotonergic migration due to the secretion of reelin (Shehabeldin et al., 2018).

Reelin controls many properties of brain development and function by controlling parts of the migration and positioning of the serotonergic neurons. Reelin is involved in the signaling process by binding to two transmembrane receptors called apolipoprotein E receptor 2 (ApoER2) and the Very Low-Density Lipoprotein Receptor (VLDLR). These receptors will then locate an adaptor protein called disabled 1 (Dab1). The receptors will initiate tyrosine phosphorylation of the five tyrosine residues on Dab1 and allow Dab1 to bind to the receptors intracellularly (Jossin et al., 2003). The ApoER2 and VLDLR receptors are found on migrating neurons and radial glial cells that will act as a transport system for moving cells. When reelin binds to both ApoER2 and VLDLR receptors and Dab1 is bound, a family of kinases (Src family) transmits the signal and triggers a cascade for neuronal connections and migration through the phosphorylation of the tyrosine kinase receptor (Shehabeldin et al., 2018). Studies have shown that reelin signaling is not only important with the migration of rostral raphe nuclei but also has shown that without reelin signaling, there is a malformation of paramedian raphe nuclei and the lateral wings of dorsal raphe nuclei. Such malformation alters the serotonergic neuronal projections and may be correlated with low-reelin level neurodevelopmental disorders, such as autism. It is still unclear

what causes disruption in reelin secretion, but a connection may be found within excess levels of serotonin or disruption in its regulation

Serotonin Transporters

Serotonin transporters are largely considered the foremost regulators of synaptic serotonin concentration during serotonergic signaling (Daws and Gould, 2011; Houwing et al., 2017). They are members of a large family of transporters called neurotransmitter sodium symporter (NSS). These symporters are responsible for the transport and reuptake of neurotransmitters through the use of sodium and chloride (Coleman et al., 2016). It is through this regulation that 5-HT can build synaptic connections and control neuronal migration and organization in early development. During adulthood, these transporters are continually used in regulation of mood and behavior (Houwing et al., 2017). However, it has been shown that serotonin transporters are expressed more during early development than in adulthood which indicates that SERT has more of a regulatory process in neuronal connections than it does in relation to mood later in life (Daws and Gould, 2011). We see the first development of serotonin transporters at gestational week 8 in the cortical analae. It is not until week 10 that the transporters arrive at the subplate and week 13 at the cortical plate. (Daws and Gould, 2011). Regardless of the stage in development, serotonin transporters and NSSs functions are dependent on many factors such as extracellular sodium, chloride, and intracellular potassium. Specifically, serotonin transporters are dependent on the sodium concentration gradient that is formed by Na+/K+ ATPases. These maintain extracellular concentrations of sodium while also keeping intracellular potassium stable. The way SERTs function is by binding sodium to serotonin transporter while simultaneously binding 5-HT (in a pronated form) and chloride. With

serotonin, chloride, and sodium all bound to the transporter, it undergoes a conformational change which orients the transporter from facing extracellularly to intracellular and releases the ions and serotonin. Intracellular potassium binds to the transporter and reorients the structure back to its normal position and allows it to work again (Figure 5) (Hellsberg et al., 2019). When serotonin transporters are disrupted, 5-HT fibers are shown to be significantly increased within the cortical layers. Going further, Garcia et al. looked at levels of reelin-positive cells due to 5-HT fibers making synaptic connections with CR cells (2019). It was observed that as 5-HT increased extracellularly due to the absence of serotonin transporters, reelin-positive cells were significantly lower (Garcia et al., 2019). Thus, without the serotonin transporter, reelin-positive cells were altered indicating that the serotonin transporter and possibly level of serotonin may be responsible for the regulation of reelin release of the Cajal-Retzius cells in the marginal zone.

Serotonin Receptors

The neurotransmitter serotonin is involved in such a large amount of regulation and developmental functions that it influences almost all of the areas of the brain (Ciranna, 2006). At first, many believed that serotonin only had two main classes of receptors called 5-HT_1 and 5-HT_2 which displays nanomolar and micromolar affinity for 5-HT (Ciranna, 2006). However, it has now been shown that there are five other serotonin receptors called 5-HT_3, 5-HT_4, 5-HT_5, 5-HT_6, and 5-HT_7. The receptors can be divided into two groups; the ligand-gated associated and the G-protein coupled associated families (Shih et al., 1995) The ligand-gated family of 5-HT receptors contains only the 5-HT_3 receptor and is the most unique of all. This receptor is considered a serotonin-gated cation channel and has the capacity to rapidly depolarize neurons (Frazer and Hensler, 1999).

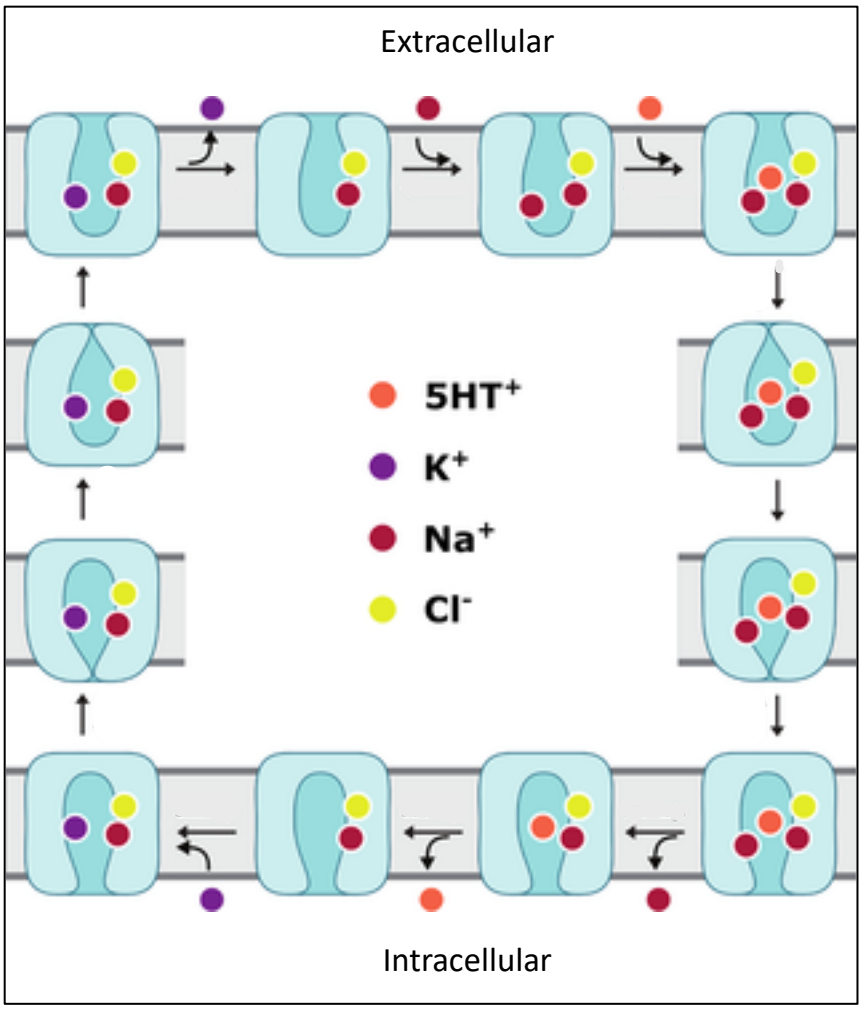

Figure 5 | Schematic representation of the serotonin transporter mechanism. An out-ward conformation of SERT bound by chloride (Cl^-) and sodium (Na^+) allows a second Na^+ molecule to bind to the complex along with extracellular serotonin ($5\text{-}HT^+$). Upon the binding of these compounds, SERT will undergo a conformation change resulting in an in-ward conformation. $5\text{-}HT^+$ and one Na^+ molecules will be release intracellularly while potassium (K^+) enters the complex. Potassium will induce another conformational change back to the out-ward position releasing K^+ and continuing the cycle again (Hellsberg et al., 2019).

In early development, the 5-HT_3 receptor can be found on GABAergic interneurons which regulate neuronal excitability. However, they have also been discovered on specific glutamatergic neurons such as the Cajal-Retizus (CR) cells in the cortex. Although the role of 5-HT_3 receptors on CR cells have yet to be elucidated, it is proposed that it may help regulate morphology, positioning, and connectivity of neurons during development (Engel, 2013). The second family of 5-HT receptors can be classified as G-protein coupled receptors (Shih et al., 1995). This family contains the rest of the 5-HT receptors and their subtypes. They too can be divided into four subfamilies. The first subfamily is the 5-HT_1 receptors. These receptors are categorized by their negative coupling of adenylyl cyclase and their capability to inhibit the activity of it. The most notable of the subtypes in this family is the 5-HT_{1A} receptor. This receptor is coupled to two effector systems which include the inhibition of adenylyl cyclase activity but also the opening of potassium channels (Frazer, 1999). It is important to note that in the dorsal raphe nuclei this receptor is only coupled to the opening of the potassium channels and does not inhibit adenylyl cyclase thus aiding in serotonin transportation (Frazer and Hensler, 1999). The second subfamily of the G-protein coupled receptors is the 5-HT_2 receptors. This group is characterized by their ability to stimulate phosphoinositide-specific phospholipase C (PI-PLC) within the cerebral cortex and is known to play a role in neuronal excitation and cell metabolism in adults (Frazer, 1999; Pithadia and Jain, 2009). The final family of 5-HT receptors is the 5-$HT_{4/6/7}$ receptors. These receptors have the opposite effects from 5-HT_1 receptor and stimulate adenylyl cyclase specifically in the hippocampus. The 5-HT_4 receptor will stimulate neuronal excitation whereas 5-HT_6 receptors will modulate acetylcholine release throughout development (Pithadia and Jain, 2009; Frazer and Hensler, 1999). These receptors have a wide range of activity but are main regulators of serotonin and other neurotransmitters throughout the

body, most notably the neurotransmitters glutamate and gamma aminobutyric acid (GABA) which have connections to the secretion of reelin and serotonergic receptors.

Glutamate and GABA Neurotransmitters

It has been reported that high levels of developmental serotonin have been associated with neurological disorders and defects in neuronal migration in early development (McNamara, 2007). During the process of development, neurons travel from the subventricular zone to the cortical plate forming a system of layers in the neocortex (Swenson, 2006). When exposed to high levels of serotonin early in development, neuronal migration begins to slow down and becomes disorganized (Brummelte, 2017). These high levels of serotonin also disrupt the extracellular matrix protein reelin which is known to aid in migration, regulation, and termination of neurons. It is still unclear how excess levels of serotonin regulate reelin secretion from Cajal-Retizus cells, but the glutamatergic and GABAergic pathways may help elucidate this phenomenon.

Glutamate and GABA are considered two of the most major neurotransmitters of the brain, working together to control many processes through excitation and inhibition of neurons. A balance between these neurotransmitters creates a homeostasis within the brain and allows normal physiology and development. However, an imbalance in both glutamatergic and GABAergic pathways can lead to diseases with known imbalances to be associated with ASD (Hampe et al., 2017).

During development, both glutamatergic and GABAergic neurons are scattered throughout the central nervous system. Glutamatergic neurons function as the excitatory role within the development of the CNS and are known to have key roles in neuronal migration,

synaptogenesis, and synaptic plasticity. However, GABAergic neurons will function as inhibitory roles throughout adulthood but has been seen to play an excitatory role in early development acting on synaptic and network levels but also cell cycle and migration (Hampe et al., 2017). This is due to elevated intracellular chloride levels during the early stages of development. Over time, these levels of chloride concentrations decrease intracellularly, and GABA shifts from a partial excitatory effect to a full inhibitory creating a homeostatic relationship with glutamate. In order for a balance to occur in early development, GABA plays a regulatory role on two types of receptors; ionotropic $GABA_a$ and metabotropic $GABA_b$ (Hampe et al., 2017).

During early development, $GABA_A$ receptors are involved in activation of calcium sensitive signaling which will lead to the excitatory role. Activation of $GABA_A$ receptors typically undergo a calcium influx resulting in depolarization. Conversely, $GABA_B$ receptors are predominantly involved in the reduction of calcium concentrations, increased neurotransmitter release, and prolonged neuronal hyperpolarization resulting in inhibitory effects. Thus, both receptors act as a balance between the excitatory and inhibitory roles during the early stages of development (Galanopoulou, 2008; Gaiarsa and Porcher, 2013; Wu and Sun, 2015; Hampe et al., 2017).

During early stages of development, it is thought that glutamate binds to the mGluta receptor found on GABAergic cells. This activation will release GABA which will bind to $GABA_A$ or $GABA_B$ receptors (Cosgrove, 2012). When bound to the $GABA_A$ receptor found on Cajal-Retizus cells it stimulates the secretion of reelin (Ciranna, 2006). This form of feedback loop between glutamate and GABA regulates the amount of reelin produced. However, the regulation of glutamate and GABA is also completed by the release of serotonin.

Serotonergic Connection with GABA/Glutamate

The serotonin receptors are complex in nature and much is still unclear on how much they govern within development. However, we do know that serotonin receptors are found on many cells including both GABAergic and glutamatergic. These receptors will act to excite or inhibit the release of glutamate through both direct termination of 5-HT neurons on glutamatergic pyramidal neurons or indirectly by GABAergic inhibitory interneurons (Stahl, 2015). Regardless of where the serotonin receptors are located, they will either be excitatory (eg, 5-HT_{2A}, 5-HT_{2C}, 5-HT_4, 5-HT_6, and 5-HT_7) or they will be inhibitory (eg, 5-HT_{1A} and 5-HT_5).

Two of the receptors have been studied extensively and their roles in neurotransmitter release has been made a bit clearer. The 5-HT_1 and 5-HT_2 receptors play opposite roles in the activity of pyramidal neurons. Activation of the 5-HT_1 receptor inhibits the release of not only more serotonin within the raphe nuclei but also inhibits glutamate release when activated on glutamatergic neurons. Conversely, activation of 5-HT_2 receptors releases glutamate on the same neurons (Maura et al., 2009; Li and Bayliss, 1998; Ciranna, 2006). When excitatory 5-HT receptors are activated on GABAergic neurons, excitation of GABA will occur which releases the neurotransmitter and inhibits the release of glutamate. Thus, serotonin aids in the regulation of both GABA and glutamate during early development. However, the receptor that serotonin binds with at a given time is still unclear. It is believed that activation of serotonin receptors depends on the receptor subtype, serotonin's affinity to a receptor, and the local concentration at a given site. For example, 5-HT_{1A} receptor has a greater affinity than 5-HT_{2A}. At low concentrations of 5-HT, the 5-HT_{1A} receptor will most likely bind with 5-HT and cause an inhibitory effect. This is not always the case and more research is needed to understand the underlying mechanisms.

In contrast, during hyperserotonemia increased activation of serotonin receptors occur. During this time, 5-HT_{2B} receptors will invoke a hyperpolarization of serotonin transporters which decreases the efficacy of SERT release of serotonin intracellularly (Baudry et al., 2019). This causes extracellular serotonin to increase and as concentrations of serotonin increase extracellularly, increased binding can occur throughout the serotonin receptors. It is hypothesized that as more receptors are activated, many will negate each other's excitatory or inhibitory responses. However, research with selective serotonin reuptake inhibitors revealed that with increased extracellular serotonin, an inhibition of glutamate release occurs more often. Additionally, the 5-HT_2 receptors are thought to also regulate which GABA receptor is activated through the phosphorylation of the $GABA_A$ receptor (Yan, 2002). When 5-HT_2 receptors are activated, the $GABA_A$ receptor currents are inhibited which causes $GABA_B$ receptors to activate instead, leading to a greater inhibitory effect on glutamate and neurotransmitter release. These findings suggest that during high levels of serotonin, serotonin transporters will decrease in efficacy leading to an increase in extracellular serotonin. With more serotonin able to bind to serotonin receptors on glutamatergic and GABAergic neurons, $GABA_A$ receptor currents will close resulting in decreased reelin. Additionally, excitation of GABAergic neurons along with inhibition of glutamatergic neurons will result in an overall decrease in glutamate release. However, more research is needed to further elucidate these mechanisms (Figure 6).

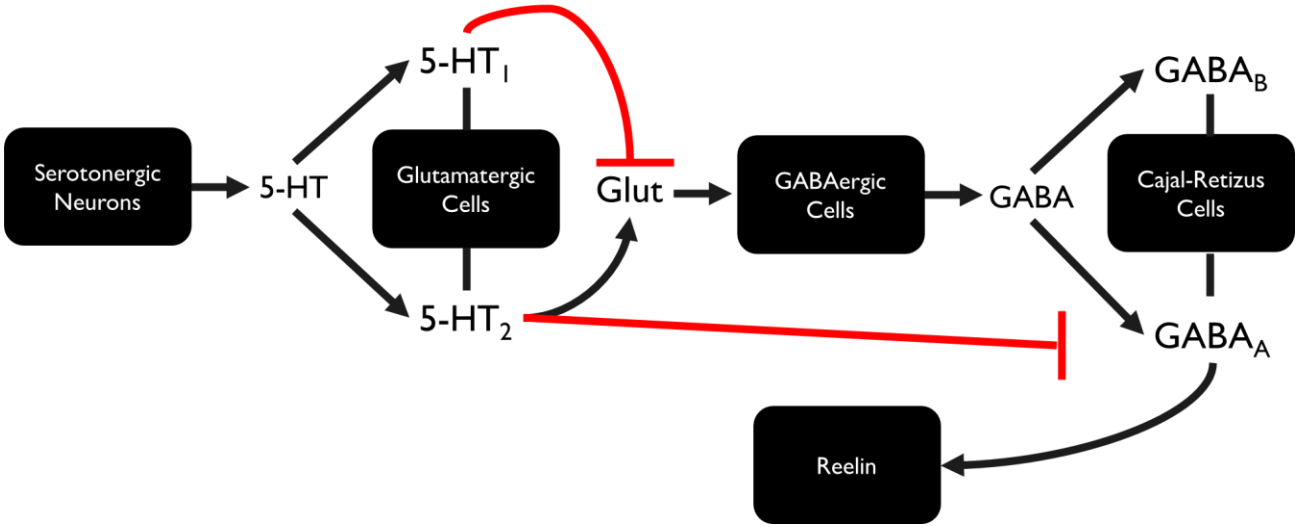

Figure 6 | Proposed developmental mechanism of neurotransmitters on reelin release. As serotonin is released extracellularly, the serotonin will bind to serotonergic receptors on glutamatergic cells which will either excite or inhibit the release of glutamate. With glutamate released, it will excite GABAergic cells to release GABA and allow $GABA_a$ receptors to be activated resulting in release of reelin. However, at the same time, serotonergic receptors can also inhibit the activation of $GABA_a$ receptor resulting in a decrease of reelin release.

AIMS & HYPOTHESIS

This project was designed to provide preliminary steps which would allow for future investigation of raphe nuclei neuronal migration in the DHS (developmental hyperserotonemia) induced Sprague Dawley rat model. Four specific aims were addressed in this work. The first aim was to identify the region of the dorsal raphe nucleus among coronal brainstem sections of a rat model. This aim was addressed via a cresyl violet staining experiment in which coronal sections of a rat brainstem was stained and visualized. It was hypothesized that utilizing nissil staining tissue histology, and known landmarks near the dorsal raphe nuclei, we could reliably and reproducibly identify of the region known to be involved in neuronal migration. Reliable identification of a diffuse subcortical neuronal population will allow for further investigation of serotonin induced neuronal migratory patterns. This complex nuclear group is involved with the earliest onset of neuronal development and contains proteins involved with both serotonergic and glutamatergic systems. Thus, correct identification of the dorsal raphe nuclei is necessary to study the relationship between serotonin and glutamate during this developmental period.

The second aim was to create an immunohistochemistry assay to label the vesicular glutamate transporter to observe levels of the neurotransmitter glutamate within the raphe nuclei. This aim was addressed by obtaining antibodies for three vesicular glutamate transporters (Vglut1-3) and optimizing immunolabeling techniques and protocols for identifying and observing the vesicular glutamate transporter surface proteins in tissue sections. It was hypothesized that primary antibodies for each of the vesicular glutamate transporters along with their respective secondary antibodies would allow for visualization of three separate wavelength

emissions. If the correct antibodies were chosen, then it will result in labeling of all glutamate transporters in the raphe nuclei and allow for distinction of each transporter group with the goal of statistical analysis in later experiments.

The third aim of this project was to develop a method to maximize the efficacy of locating the dorsal raphe nuclei and labeling the vesicular glutamate transporters reliably and reproducibly. This aim was addressed by optimizing protocols in aim 1 and 2 for cresyl violet staining of the dorsal raphe nuclei and immunohistochemistry for labeling vesicular glutamate transporters. With methods developed, aim three allowed for qualitative analysis of histological samples using laser scanning confocal microscopy. It was hypothesized that with an optimized protocol, future investigations could utilize the methods and minimize the time, numbers of animals, costly antibodies, and necessary reagents when conducting analytical research on vesicular glutamate transporters in the dorsal raphe nuclei.

The last aim was to evaluate the effects of DHS on vesicular glutamate transporter in the raphe nuclei on Sprague Dawley rat populations when compared to saline treated controls. This aim was postponed due to time constraints and COVID induced obstacles yet would have been addressed by analyzing raphe nuclei sections from DHS- and saline controlled rats, with vesicular glutamate transporter labeled using the previous IHC protocol and visualized using confocal microscopy and ImageJ software. It was hypothesized that excess levels of serotonin will activate 5-HT receptors that will provide an overall inhibitory effect on glutamate release.

MATERIALS & METHODS

Experimental Animals

Timed-pregnant Sprague Dawley rats were previously purchased from Charles River Laboratories and subject to daily subcutaneous injections. Two of the four pregnant dams were selected to receive daily injections of 5-methoxytrypatamine (5-MT) solution whereas the remaining two were administered saline solutions as a control. Pups were born from the four rats and were subject to subcutaneous injections as well. Pups born from the dams with 5-MT injections were subject to daily 5-MT injections whereas the pups born from saline treated rats were administered saline solutions on a daily basis.

Injection Preparation and Administration

Protocol for the injection and administration of 5-MT and saline solutions were modified from the experimental procedure created by Whitaker-Azmitita (2001) for the animal developmental hyperserotonemia model of ASD in Sprague-Dawley rats. In order to replicate the 50% increase in serotonin commonly found within ASD patients, a dosage of 1.0 mg/kg of animal body weight was kept consistent throughout the administrating period (Whitaker-Azmitita, 2005).

The 5-MT solution was created with a concentration of 1 mg/mL of granular 5-MT (Sigma Aldrich, Cat. No 286583) within an 85% saline solution (Ricca Chemical Company, Cat No. 7200-32). The mixture was vortexed until dissolved and stored at -20˚C until administration.

The injected saline solution was comprised of 85% saline solution (Ricca Chemical Company, Cat No. 7200-32) with no further alterations.

Administration of the 5-MT and saline solutions were conducted in a dimly lit room to minimize the degradation of the agonist, 5-MT. Each day, experimental and control dams were subject to injections between 10:00 am – 12:00 pm CST of their respective solutions. This was consistent from gestational day 12 until delivery of rat pups. From here, the pups were subject to subcutaneous injections corresponding that that of their originating dam. In order to reduce stress of the rats, the solution was warmed to 40℃ before injections and administered the scruff of the neck while being held firmly.

Tissue Collection and Fixation

The dams were euthanized on post-natal day 21 while away from the pups to reduce stress. The subsequent pups underwent motor behavioral training and testing from PND 21 until PND 28. After testing occurred, the pups were euthanized through whole-animal perfusion with 4% paraformaldehyde. Pups were anesthetized with 2-4% isoflurane gas at 1-2 L/min until unresponsive. Trans-cardial perfusion was performed with ice-cold saline followed by 4% paraformaldehyde. A small transverse incision was created at the base of the skull with a razor blade to peel back the muscle. The cervical vertebra was then severed before horizontal incisions were created at the foramen magnum. Rongeurs were used to remove the calvarium before severing the olfactory bulb and cranial nerves from the ventral surface of the brain. The intact brain tissue was removed and fixated in conical vials containing 4% paraformaldehyde and stored at 4ºC.

Cryosectioning

Previously harvested intact brain samples from Sprague Dawley rats were stored within conical vials containing 4% paraformaldehyde at 4°C. Control wildtype tissue samples were cut using a single edge industrial razor blade to separate the brainstem from the cortex and cerebellum with the caudal diencephalon kept intact using gross neuroanatomical landmarks as reference. The tissue samples were placed in a sucrose solution and stored at 4°C. After a minimum of 48 hours or upon complete submersion of tissue samples in the sucrose solution, the tissue samples were taken out of the sucrose solution and blotted with Kimberly-Clark Kimwipes to remove any excess superficial sucrose crystals. The sections were placed on a specimen stage and left directly inside the Thermo Microm HM550 Cryostat for a minimum of one hour at -20°C. The remaining sections were returned to the sucrose solution and stored at 4°C. After one hour, the tissue samples were embedded in optimal cutting temperature (OCT) compound (Fisher Cat No. 23-730-571) and left to solidify. Continual application of OCT was conducted until the tissue sample was completely covered. The specimen stage was added to the docking station of the cryostat and a single, disposable, high profile microtome blade (Fisher Cat No. 31-517-35) was inserted and locked into place at an 8° angle. The glass cover slip was released and set aside while the cryostat was set to trim 70 μm sections. The OCT surrounding the tissue sample was trimmed until sections of the tissue were seen. The cryostat was adjusted to fine sections of 30 μm and sectioning continued. Using a sterilized pinpoint tweezer, free floating 30 μm tissue sections were carefully placed inside a 24-well cell culture plate (CellStar Cat No. 622 160) filled with 1000 μL of 25mM PBS solution. Each well contained one individual 30 μm section.

Cryosectioning continued until no tissue sample was left on the specimen stage. Collections of samples were labeled and stored in 4°C until undergoing cresyl violet staining.

Cresyl Violet Staining and Mounting

The following cresyl violet staining procedure was conducted utilizing 24-well cell culture plates (CellStar Cat No. 622 160) containing free-floating coronal brainstem sections. To begin, a cresyl violet solution containing 0.1g cresyl violet, 250uL glacial acetic acid (0.25% v/v) and 100mL of ddH_2O was mixed overnight, vacuum filtrated, and stored in a dark, dry environment before use. Free-floating 30 μm sections were washed with 1000 μL of 25mM PBS for five minutes, three consecutive times. Sections were then dehydrated by incubating in ddH_2O for five minutes. Once dehydrated, the samples were incubated in 1000 μL of cresyl violet solution for ten minutes at room temperature while rocking. Sections were washed with 1000 μL of ddH_2O for five minutes, twice. Sections were removed from the 24-well culture plates and rolled onto a Superfrost®Plus microscope slides that were positively charged using a sterilized paintbrush. Each slide contained four individual 30 μm sections. Kimberly-Clark Kimwipes were used to absorb excess ddH_2O from the slides before being placed in an oven for 1-5 minutes or until tissues were fixed. Once the slides were dry and samples fixated, samples were washed with 1000 μL of 90% ethanol with acetic acid by allowing the solution to run across the slide in a dropwise manner (Figure 7). A second wash was conducted with 3000 μL of 90% ethanol in the same dropwise manner. Sections were then washed with 3000 μL of 95% ethanol followed by washing with 3000 μL of 100% ethanol, twice. Once the wash was completed, sections were introduced to 3000 μL of 100% xylene in the same manner, three consecutive times. Slides were then mounted by adding a drop of Permount (Fisher Cat No. SP15-100) to each slide's end with a glass pipette and dragged across the middle of the slide to ensure a thin line of Permount was

across the entire slide. A #1.5 24x6 mm coverslip (Fisherbrand) was quickly added to the slide at a 45° angle while keeping enough pressure to spread the Permount across the slide without

Figure 7 | Cresyl Violet Wash Method. During the washing steps of cresyl violet protocol, instead of submerging the slides with adhered tissues, a 45-degree angle was made where wash solutions could flow down the slide and over the tissue samples.

bubbles forming. Slides with coverslips were placed in a fume hood to dry and seal before observation under a microscope.

Vibratome Sectioning

Before conducting sectioning of tissue, 75% ethanol was sprayed onto a cutting board and the Vibratome Series 3000 to disinfect. The previously harvested sprague-dawley rat brain samples that were stored at 4˚C in 4% paraformaldehyde were retrieved and placed onto the cutting board. The brain samples were cut using a single edge industrial razor blade to separate the brainstem from the cortex and cerebellum with the caudal diencephalon kept intact. The brainstem was kept as the remaining tissue samples were returned to the 4% paraformaldehyde and stored in 4˚C.

A 4% agarose was created in liquid form by using 25mM PBS and heating it until clear. The molten agarose was then poured into a 15x15x15 disposable base mold (Fisherbrand Cat No. 22-363-553) and allowed to cool slightly but not solidify. Once cooled to the touch, the brainstem section was placed into the base mold/molten agarose with the rostral portion of the brainstem placed on the bottom of the mold. The molten agarose surrounded the brainstem sample aside from portions of the exposed caudal end. The agarose was then left to cool until solid. The embedded tissue was removed from the base mold and trimmed using a single edge razor blade. The prepared tissue sample in agarose was fixed to a metal platform with cyanoacrylate with the exposed caudal portion of the brainstem facing upward. Once the adhesive dried the metal platform was tightened into the Vibratome Series 3000 specimen mount position in a way that the blade would fully cut through the mold.

An uncoated, disposable vibratome injector blade was loaded into the spring clamp at a 15˚ angle. The vibratome's speed was then set to 2 and the amplitude set to 8. The platform's height was adjusted so that the top of the agarose mold would be level with the injector blade. The specimen bath was then filled with 25mM of PBS so that the mold and the injector blade had a thin layer of liquid covering them.

The Vibratome Series 3000 was set to manual mode and started. The exposed caudal section of the brainstem was cut off before carrying out sample collection. Once cut, the dial was turned as to cut 50 um coronal sections and allowed to proceed. The coronal section was removed from the specimen bath using a sterilized paint brush and separated from the agarose mold. The tissue section was placed into a 24-well culture plate containing approximately 1000 uL of 25mM PBS. Steps were repeated adjusting the dial for 50 um and sample collection until the brainstem sample was completely cut. The sections were placed in 4˚C until undergoing immunohistochemistry staining for visualization of vesicular glutamate transporters.

Immunohistochemistry and Mounting

The following immunohistochemistry (IHC) protocol was optimized utilizing previously tested IHC methods from Hough Lab. The entire protocol was conducted using coronal brainstem sections at a thickness of 50 um free floating in 24-well culture plates (Fisherbrand). Free-floating sections were taken out of the 25mM PBS storage solution and incubated in 0.15 M glycine (BioRad Cat No. 161-0718) in 25mM PBS for 10 minutes at room temperature. Sections were then introduced to 300 uL of a 25mM PBS solution containing 0.05% Tween-20 (BioRad Cat No. 170-6531) along with 1% Triton-X-100 (Millipore Sigma Cat No. 9036-19-5). Sections were left to sit in this solution for one hour at room temperature. Upon returning, sections were

washed using 1000 uL of 0.05% Tween-20 in 25mM PBS, also known as “PNT buffer”. Sections were washed three times in the PNT buffer each for five minutes at room temperature. Blocking was then performed using 300 uL of a 25mM PBS solution containing 2% goat serum (Millipore Sigma Cat No. 191356), 1% bovine serum albumin (Fisher BioReagents Item No. EW-88057-64), 0.1% Triton-X-100, and 0.05% Tween-20. Sections were left to incubate in the blocking solution for one hour at room temperature while rocking. While blocking was occurring, anti-Vglut 1 primary antibody (Thermofisher Scientific Cat No. MA5-27614) received a 1:1000 dilution, anti-Vglut 2 primary antibodies (Millipore Cat No. AB2251) received a 1:1000 dilution, and anti-Vglut 3 primary antibodies (ThermoFisher Scientific Cat No. PA5-77432) received a 1:1000 dilution all within the blocking solution utilized previously. Following blocking, tissues were introduced to 300 uL of the primary antibody solution for a minimum of two days at 4˚C while rocking.

Following primary antibody incubation, tissue sections were washed with 1000 uL of PNT buffer for five minutes, twice. On a third wash, tissues were held for one hour at 4˚C while rocking. Goat anti-Mouse Alexa Fluor 488 conjugated secondary antibodies specific to anti-Vglut1 primary antibodies (ThermoFisher Scientific Cat No. A32723) received a 1:200 dilution, goat anti-guinea pig Alexa Fluor 555 conjugated secondary antibodies specific to anti-Vglut2 primary antibodies (ThermoFisher Scientific Cat No. A-21435) received a 1:200 dilution, and goat anti-rabbit Alexa Fluor 680 conjugated secondary antibodies specific to anti-Vglut3 (ThermoFisher Scientific Cat No. A32734) received a 1:200 dilution, all within the blocking solution utilized previously. Sections were incubated in 300 uL of secondary antibody solution for 24 hours at 4˚C while rocking in the dark. Sections were washed utilizing 1000 uL of PNT buffer for five minutes while rocking in the dark. Tissues were washed twice more but on the

third wash sections were held in PNT buffer for 7-12 hours. Sections were washed twice more in 1000 uL of PNT buffer for five minutes and then mounted.

The coronal brainstem sections were mounted onto positively charged SuperFrost®Plus (Fisherbrand) adhesive 1”x3” microscope slides. FluroGel II with DAPI (Electron Microscopy Sciences, Cat No. 17985-50) was added to the microscope slides dropwise and streaked across the middle of the slide. A #1.5 24x6 mm cover glass (Fisherbrand) was gently added to the slides and cleaned up using Kimberly-Clark Kimwipes. Slides were allowed to dry in the dark before being covered in aluminum foil and stored at 4˚C until imaged with confocal microscopy.

RESULTS

Identification of Dorsal Raphe Nuclei Location via Coronal Brainstem Samples of Saline Treated Rat Models

Identification of the dorsal raphe nucleus location among coronal sections of rat brainstems was investigated through the application of a cresyl violet stain followed by analysis using brightfield microscopy. Saline treated Sprague Dawley rat brain samples were randomly taken from 4% paraformaldehyde storage and stained allowing the visualization of cell nuclei, projecting fibers, and structural landmarks. The first three staining rounds resulted in coronal brainstem sections becoming unadhered to slides and becoming free floating within the staining solution (Figure 6). Due to a lack of successful results, a secondary experiment occurred to adhere the tissues samples before staining. The first of these experiments was to test the properties of the SuperFrost® Plus slides for inconsistencies (Table 1). Two types of slides were tested including SuperFrost® Plus and StarFrost® Plus slides in order to eliminate the possibility of a defective charge of the slides. Tests resulted in samples failing to be fully adhered and peeling off the two types of slides before washes were complete (Figure 6). Failure was tracked by more than 75% of the slides becoming unadhered and washing away in solutions. A following experiment tested whether duration of the adherence process of the sections would be successful (Table 2). This resulted in sections once again peeling off the slides during the wash and staining steps. Lastly, an experiment occurred where tissue sections were subject to heat via an oven for 5 or 10 minutes prior to being left out to dry (Table 3). This resulted in samples staying adhered on the slides for the longest amount of time only peeling off during the cresyl violet stain and

subsequent washes. However, based on the criteria for success and failure, ultimately this resulted in failure to adhere the tissues.

Following the secondary experiment, a new method of cresyl violet staining was conducted to prevent any unnecessary movement of the tissue samples as they were on the slides. Tissues were heat dried onto SuperFrost® Plus slides and washed with solutions using a dropper. Following repeated trials, this resulted in successful completion of the staining protocol with all tissue samples staying adhered to the slides (Table 4). However, upon analysis of the first successful stain, it was seen that overstaining had occurred where cell nuclei were unable to be differentiated from the white matter (Figure 6). Thus, further optimization and repeated testing occurred where amount of heat to fixate tissues, amount of wash, time of staining, and addition of acetic acid in 70% ethanol were tested (Table 5).

Upon successful optimization of cresyl violet staining, brainstem sections were viewed under a confocal microscope in order to visualize landmarks of the dorsal raphe nuclei (Figure 8-11). The dorsal raphe nuclei were able to be found utilizing four distinct landmarks of the coronal brainstem sections: the cerebral aqueduct along the midline, the superior colliculus along the superior edge, the pontine nuclear group inferior to the cerebral aqueduct, and the cuneiform nuclear group lateral to the cerebral aqueduct (Figure 8-11).

Table 1. Tissue Adhesion via Type of Slides

Slide Type	Fixation of Tissue Samples	
	Orientation	**Adhesion**
StarFrost® Plus	Forward	Failure
SuperFrost® Plus	Forward	Failure
StarFrost® Plus	Reverse	Failure
SuperFrost® Plus	Reverse	Failure

Table 2. Tissue Adhesion via Duration of Tissue Drying

Slide Type	Adhesion of Tissue Samples via Drying Duration		
	Orientation	**Drying Duration (Hr)**	**Adhesion**
StarFrost® Plus	Forward	48	Failure
SuperFrost® Plus	Forward	48	Failure
StarFrost® Plus	Reverse	48	Failure
SuperFrost® Plus	Reverse	48	Failure

Table 3. Tissue Adhesion via Heat and Duration

Slide Type	Adhesion of Tissue Samples via Heat			
	Orientation	Drying Duration (Hr)	Heat Fixation (min)	Adhesion
SuperFrost® Plus	Forward	48	5	Failure
SuperFrost® Plus	Forward	48	5	Failure
SuperFrost® Plus	Reverse	48	5	Failure
SuperFrost® Plus	Reverse	48	5	Failure
StarFrost® Plus	Forward	48	10	Failure
StarFrost® Plus	Forward	48	10	Failure
StarFrost® Plus	Reverse	48	10	Failure
StarFrost® Plus	Reverse	48	10	Failure

Table 4. Free Floating Tissue Adhesion Before Staining vs After Dehydration Steps

Cresyl Violet Staining via Dropwise Solutions					
Slide Type	**Orientation**	**Drying Duration (Hr)**	**Heat Fixation (min)**	**Dropwise Wash**	**Adhesion**
SuperFrost® Plus	Forward	12	5	Yes	Success
SuperFrost® Plus	Forward	12	5	Yes	Success
SuperFrost® Plus	Forward	48	10	Yes	Success
SuperFrost® Plus	Forward	48	10	Yes	Success
SuperFrost® Plus	Forward	12	5	No	Failure
SuperFrost® Plus	Forward	12	5	No	Failure
SuperFrost® Plus	Forward	48	10	No	Failure
SuperFrost® Plus	Forward	48	10	No	Failure

Table 5. Optimization of Free Floating and Dropwise Staining Method

Cresyl Violet Staining Optimization Table							
Slide Type	**Orientation**	**Drying Duration (Hr)**	**Heat Fixation (min)**	**Dropwise Wash**	**Acetic Acid Wash (sec)**	**Adhesion**	**Staining**
SuperFrost® Plus	Forward	48	5	Yes	10	Success	Success
SuperFrost® Plus	Forward	48	10	Yes	10	Success	Overstained
SuperFrost® Plus	Forward	48	10	Yes	15	Success	Success
SuperFrost® Plus	Forward	12	10	Yes	30	Success	Success
SuperFrost® Plus	Forward	12	10	Yes	0	Success	Overstained

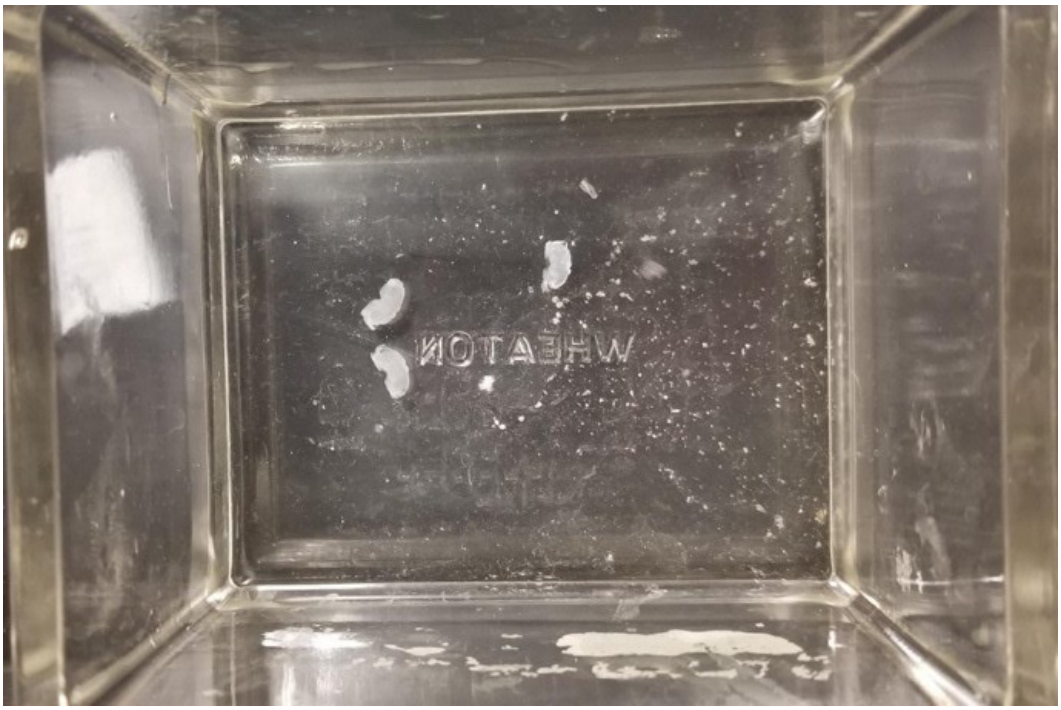

Figure 8 | Free-Floating Tissue Samples. During cresyl violet staining, tissue samples that did not adhere to the charged slides would become free floating in the wash and staining solutions as shown above. When 75% of the tissue samples became free floating, the experiment failed, was stopped, and adjusted.

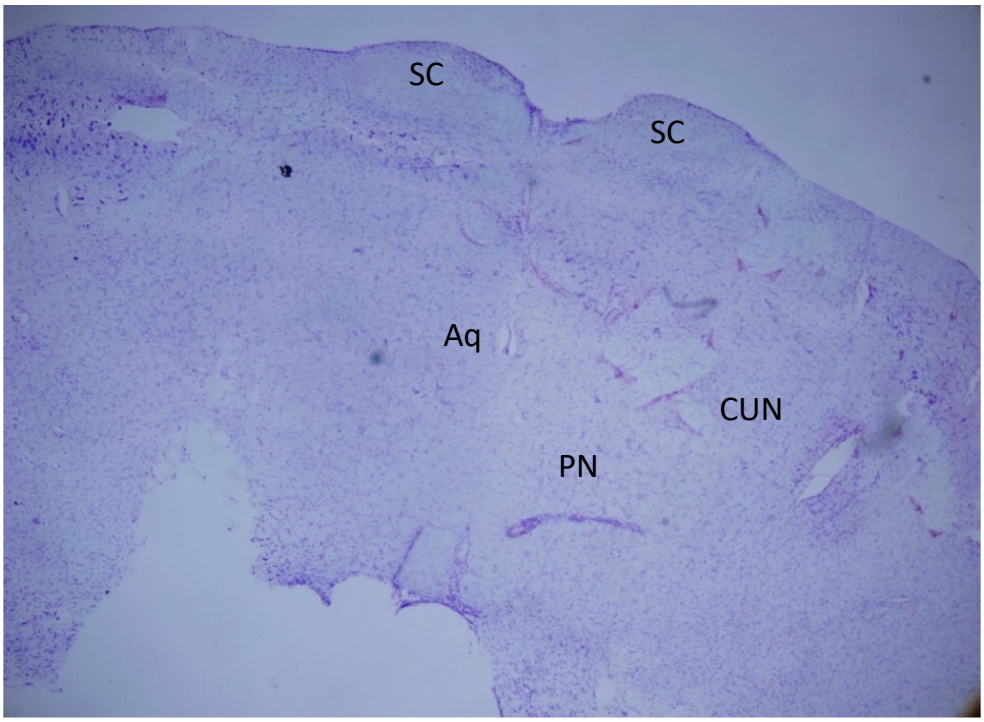

Figure 9 | 10X Magnification of a Cresyl Violet Stain of the Dorsal Raphe Nuclei. Individual landmarks of coronal brainstem sections include the superior colliculus (SC), cerebral aqueduct (Aq), pontine nuclear group (PN), and the cuneiform nuclear group (CUN).

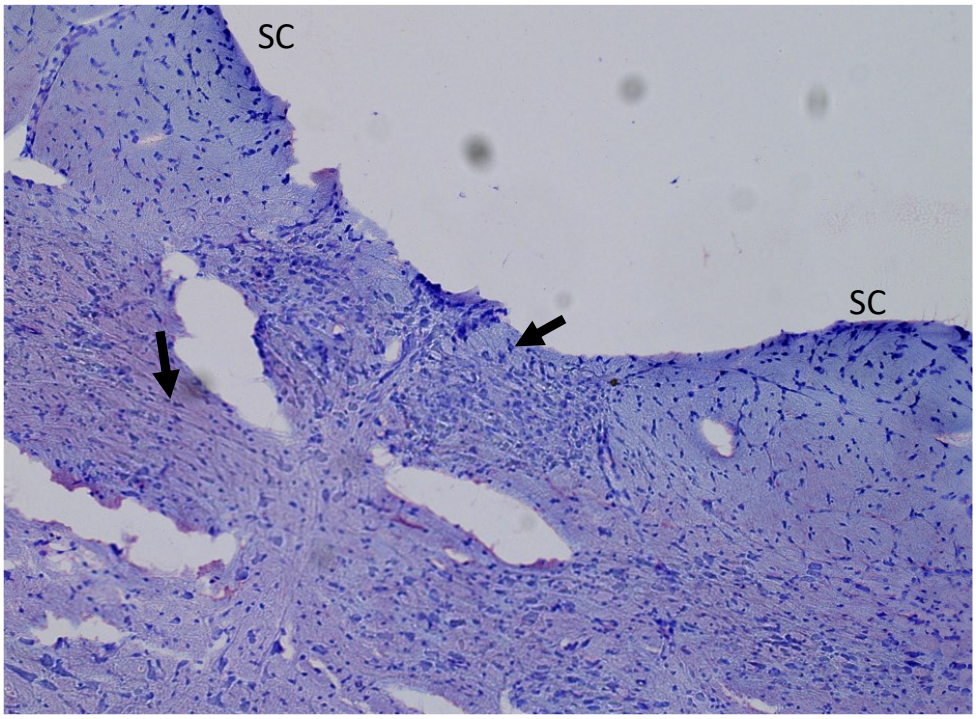

Figure 10 | 40X Magnification of a Cresyl Violet Stain of the Superior Colliculus in a Coronal Section of Rat Brainstem. Individual landmarks of coronal brainstem sections using oil immersion 40x objective lens. The superior colliculus is located at the most superior portion of the coronal section with individual nuclei bodies indicated by the arrows.

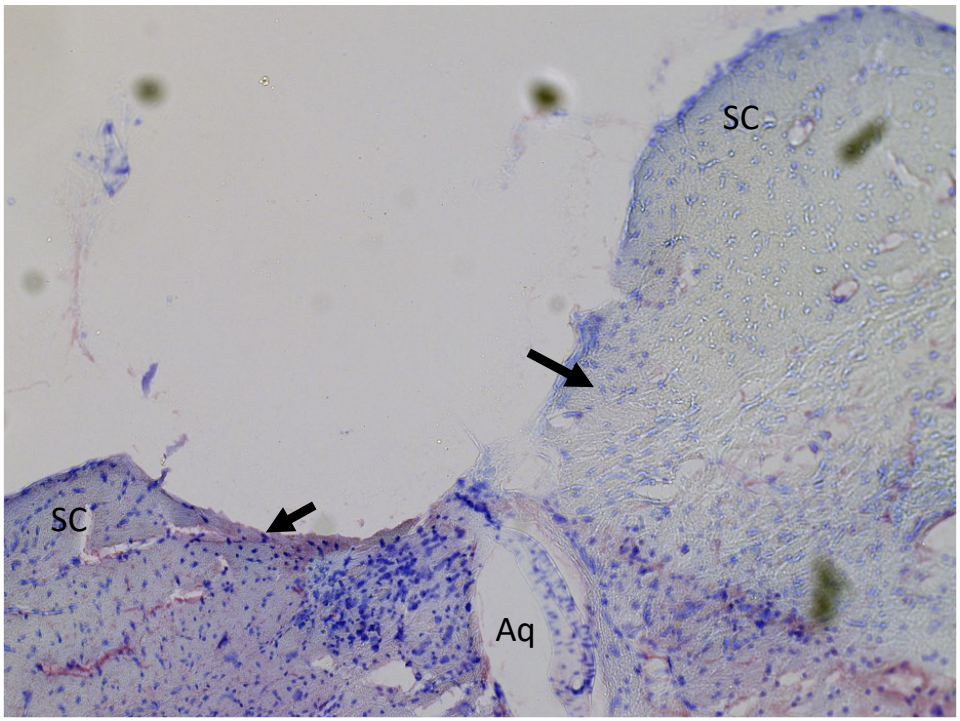

Figure 11 | 40X Magnification of a Cresyl Violet Stain of the Cerebral Aqueduct in a Coronal Section of a Rat Brainstem. Individual landmarks of coronal brainstem sections using oil immersion 40x objective lens. The superior colliculus is located at the most superior portion of the coronal section with individual nuclei bodies indicated by the arrows. The cerebral aqueduct (Aq) is located along the midline of the section indicated by the lack of nuclei bodies.

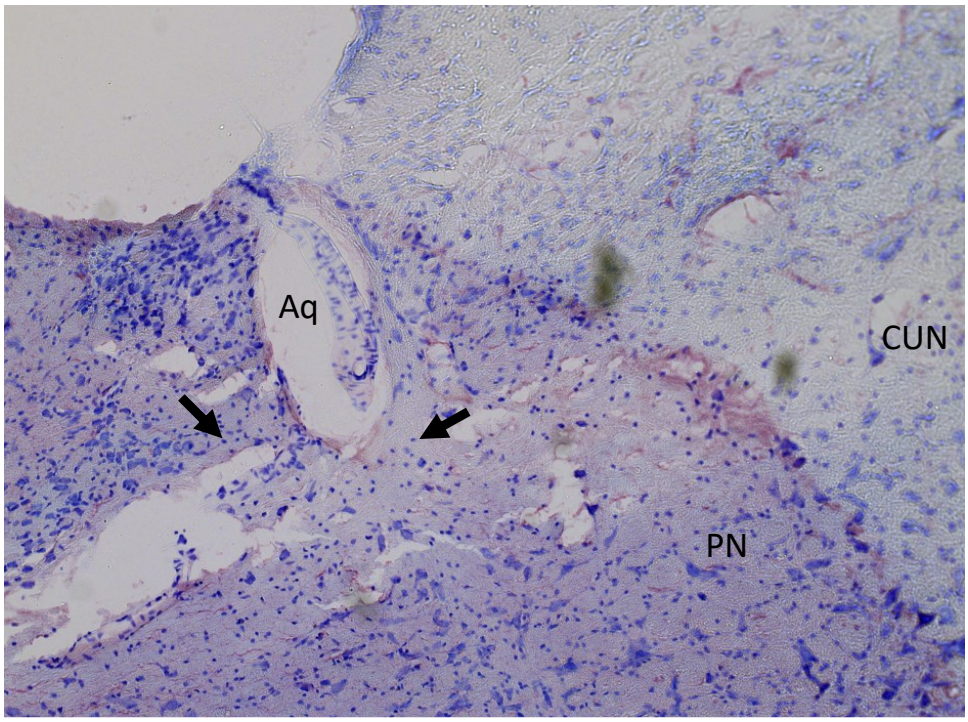

Figure 12 | 40X Magnification of a Cresyl Violet Stain of the Pontine Nuclear Group and Cuneiform Nuclear Group in a Coronal Section of a Rat Brainstem. Individual landmarks of coronal brainstem sections using oil immersion 40x objective lens. The cerebral aqueduct (Aq) is located along the midline of the section indicated by the lack of nuclei bodies. The Pontine nuclear group (PN) is located inferior to the cerebral aqueduct and lateral to the midline. The cuneiform nuclear group (CUN) is located supero-lateral to the pontine nuclear group. Individual nuclei bodies are indicated by arrows.

Visualization of Vesicular Glutamate Transporters via Immunohistochemistry

Investigation of the glutamate transporters associated with dorsal raphe nuclei was conducted via application of Immunohistochemistry followed by analysis using laser scanning confocal microscopy and ImageJ software. The glutamate transporters one through three were labeled using respective primary antibodies (ThermoFisher). Vesicular glutamate transporter 1 proteins were labeled with Mouse anti-VGlut1 antibodies, vesicular glutamate transporter 2 proteins were labeled with Guinea Pig anti-VGlut2 antibodies, and vesicular glutamate transporter 3 proteins were labeled with Rabbit anti-VGlut3 antibodies. Labeling of the vesicular glutamate transporters allowed assessment of glutamatergic presence within the dorsal raphe nuclei of rat brainstems. The fluorescently stained coronal sections were imaged, and pictures of the sections were taken with a Leica DMi8 laser scanning confocal microscope at 40X objective lens with oil immersion.

The first immunohistochemistry trials consisted of labeling vesicular glutamate transporter 2 (VGlut2) proteins within the dorsal raphe nuclei in rat brainstem tissue samples stored previously for 2 years. The following concentrations of washes and dilutions were utilized to observe complete labeling of VGlut2. The completed process resulted in high levels of background staining as the VGlut 2 proteins could not be differentiated from nuclei bodies in the dorsal raphe nuclei. Subsequent testing occurred with tissues harvested a week prior and sectioned using a vibratome at 50um. The concentrations of washes and dilutions were altered in order to lower the background emissions.

The vesicular glutamate transporter 2 proteins were labeled among the dorsal raphe nuclei with minimal background signal. Using the same concentrations, additional antibodies for vesicular glutamate transporter 1 proteins was added to the protocol. Upon observation of tissue

samples utilizing the confocal microscope, both vesicular glutamate transporters were labeled with minimum background staining. Lastly, vesicular glutamate transporter 3 protein antibodies were included with the previous two antibodies and all three vesicular glutamate transporters were labeled. Dilutions for all three antibodies were keep the same and resulted in clear fluorescent labeled with low background emissions (Figure 13-18).

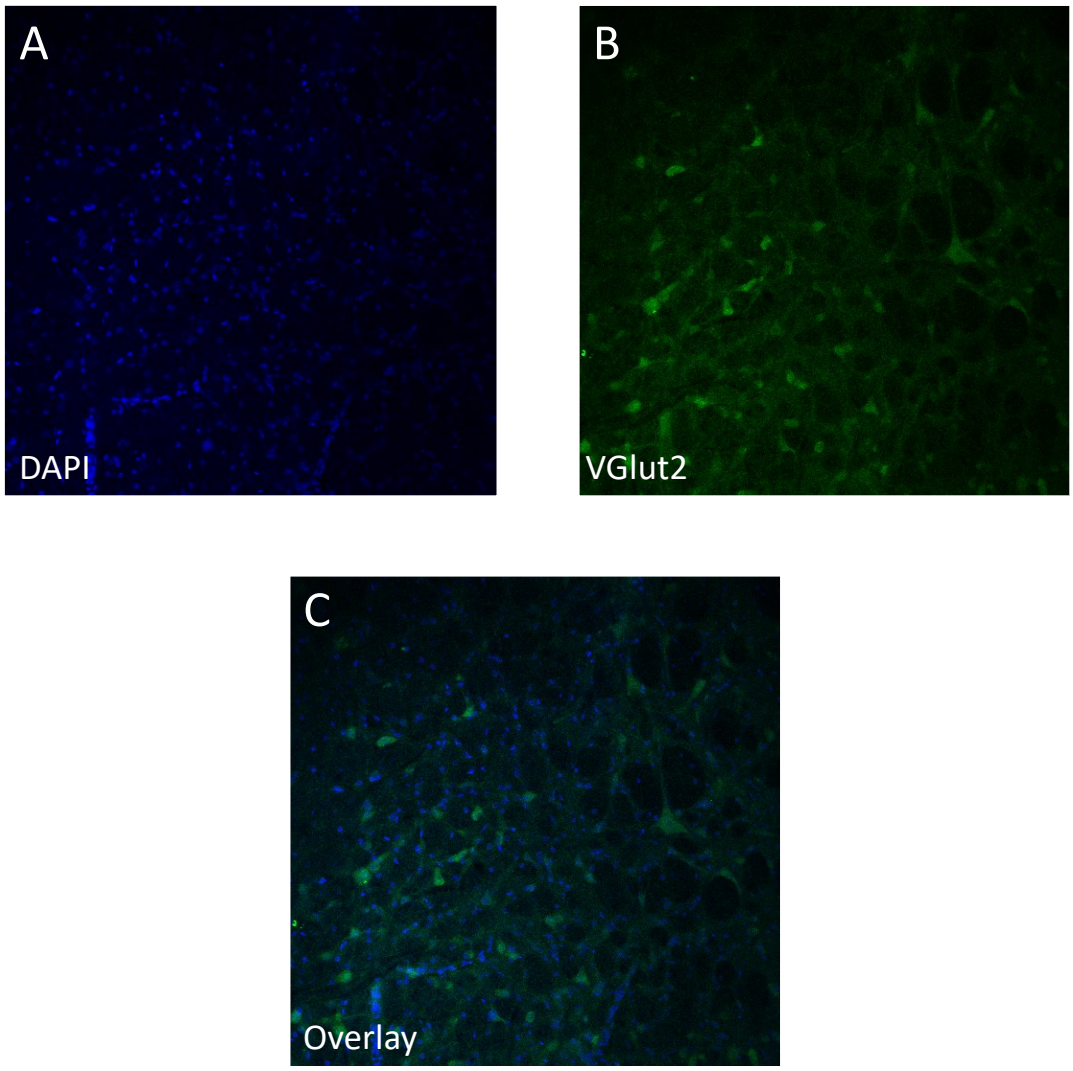

Figure 13 | Overstained Distribution of Vesicular Glutamate Transporter 2 Proteins in the Dorsal Raphe Nuclei. Sprague-Dawley rat coronal brainstem sections A6 (harvested two years prior) were imaged using a DMi8 confocal microscope at a 40x objective lens with oil immersion. (A) Cellular nuclei were stained using DAPI, shown in blue. (B) Vesicular glutamate transporter 2 proteins (VGlut2) were labeled using Alexa 488 secondary antibodies, shown in green. (C) Overlay of VGlut2 and cellular nuclei. Sections were 25 um in thickness.

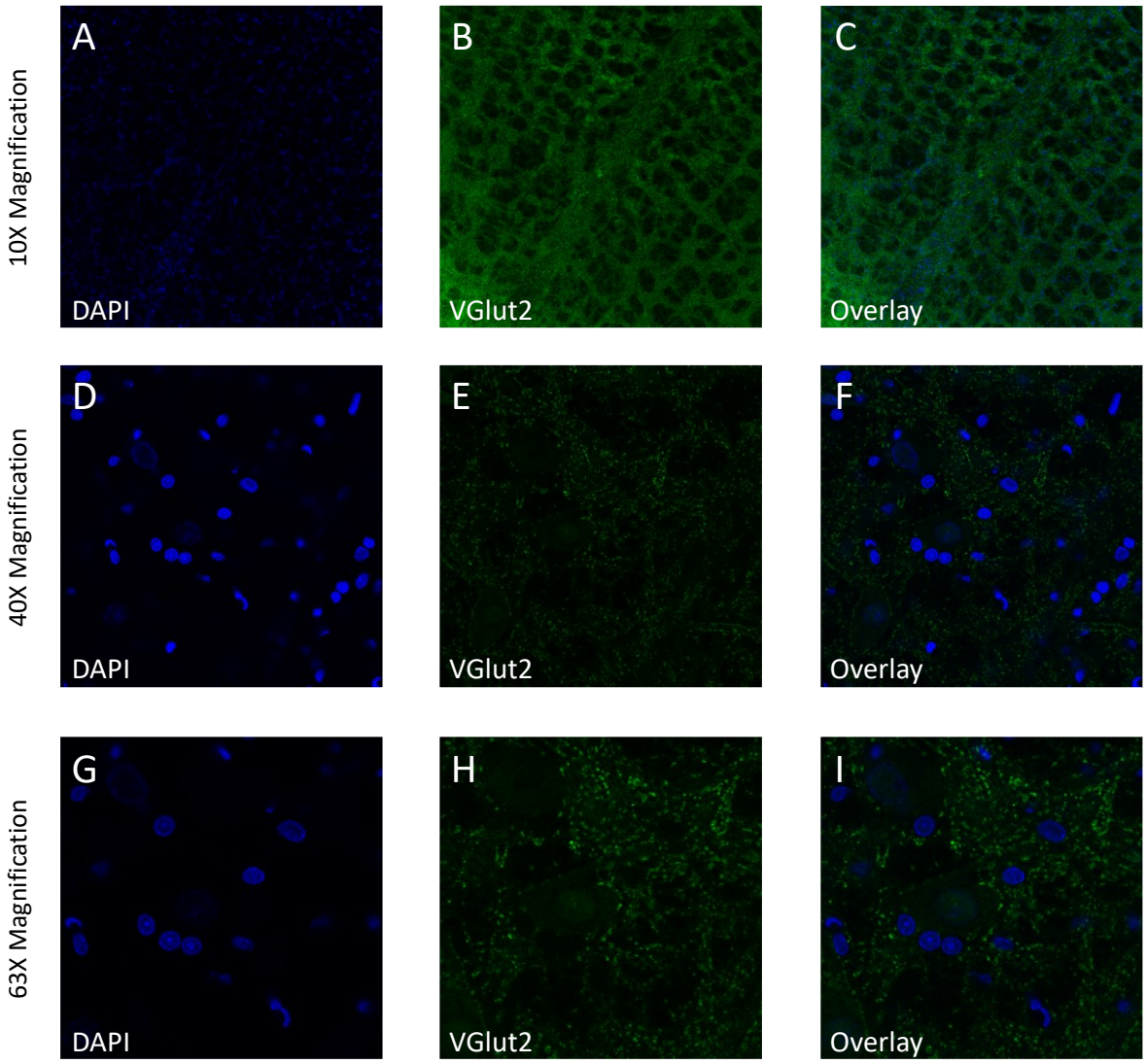

Figure 14 | Distribution of Vesicular Glutamate Transporter 2 Proteins in the Dorsal Raphe Nuclei Using Sample 3-86.5. Sprague-Dawley rat coronal brainstem sections 3-86.5 (harvested a week prior) imaged using a DMi8 confocal microscope at a 10x, 40x, and 63x objective lens with oil immersion at 40x and 63x. (A) Cellular nuclei were stained using DAPI, shown in blue. (B) Vesicular glutamate transporter 2 proteins (VGlut2) were labeled using Alexa 488 secondary antibodies, shown in green. (C) Overlay of VGlut2 and cellular nuclei. Sections were 50 um in thickness.

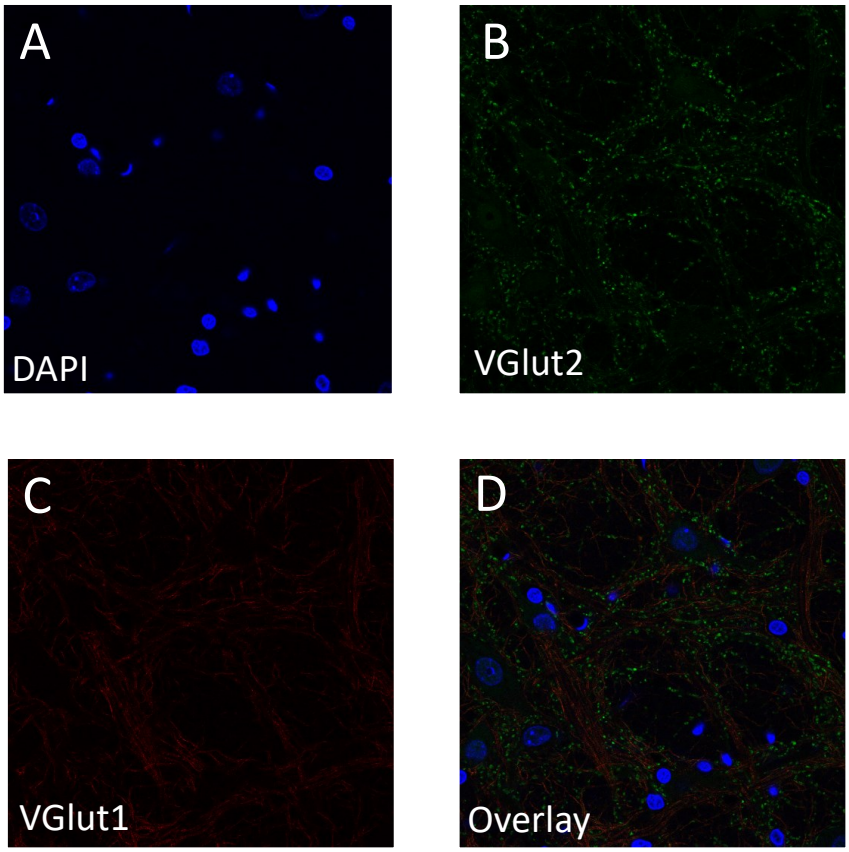

Figure 15 | 40x Magnified Expression of Vesicular Glutamate Transporter 1 and 2 Proteins in the Dorsal Raphe Nuclei Using Sample 3-86.5. Sprague-Dawley rat coronal brainstem sections 3-86.5 (harvested a week prior) imaged using a DMi8 confocal microscope at a 40x objective lens with oil immersion (A) Cellular nuclei were stained using DAPI, shown in blue. (B) Vesicular glutamate transporter 2 proteins (VGlut2) were labeled using Alexa 488 secondary antibodies, shown in green. (C) Vesicular glutamate transporter 1 proteins (VGlut1) were labeled using Alexa 555 secondary antibodies, shown in red. (D) Overlay of VGlut1, VGlut2, and cellular nuclei. Sections were 50 um in thickness.

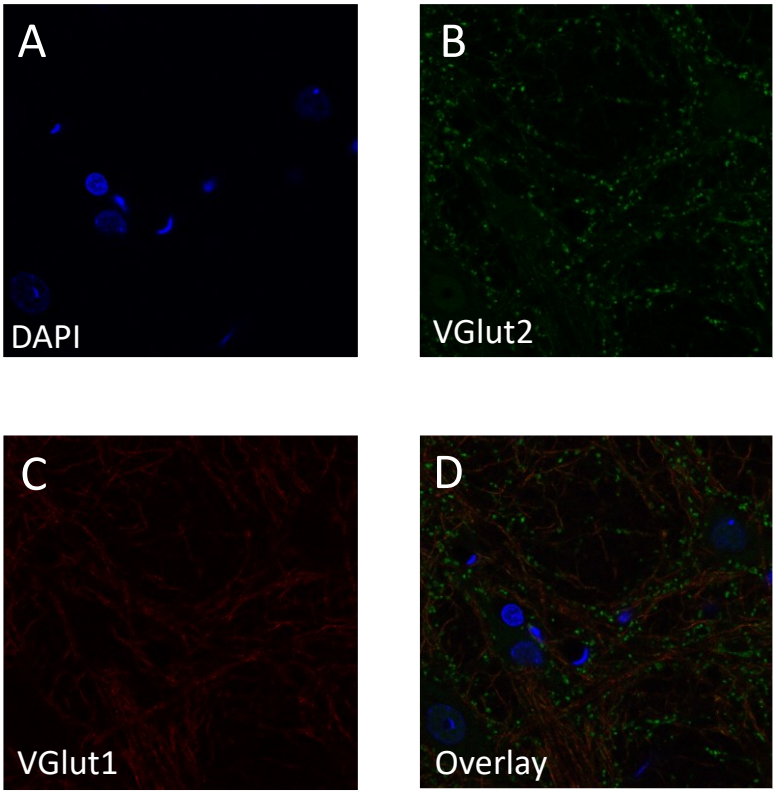

Figure 16 | 63x Magnified Expression of Vesicular Glutamate Transporter 1 and 2 Proteins in the Dorsal Raphe Nuclei Using Sample 3-86.5. Sprague-Dawley rat coronal brainstem sections 3-86.5 (harvested a week prior) imaged using a DMi8 confocal microscope at a 63x objective lens with oil immersion (A) Cellular nuclei were stained using DAPI, shown in blue. (B) Vesicular glutamate transporter 2 proteins (VGlut2) were labeled using Alexa 488 secondary antibodies, shown in green. (C) Vesicular glutamate transporter 1 proteins (VGlut1) were labeled using Alexa 555 secondary antibodies, shown in red. (D) Overlay of VGlut1, VGlut2, and cellular nuclei. Sections were 50 um in thickness.

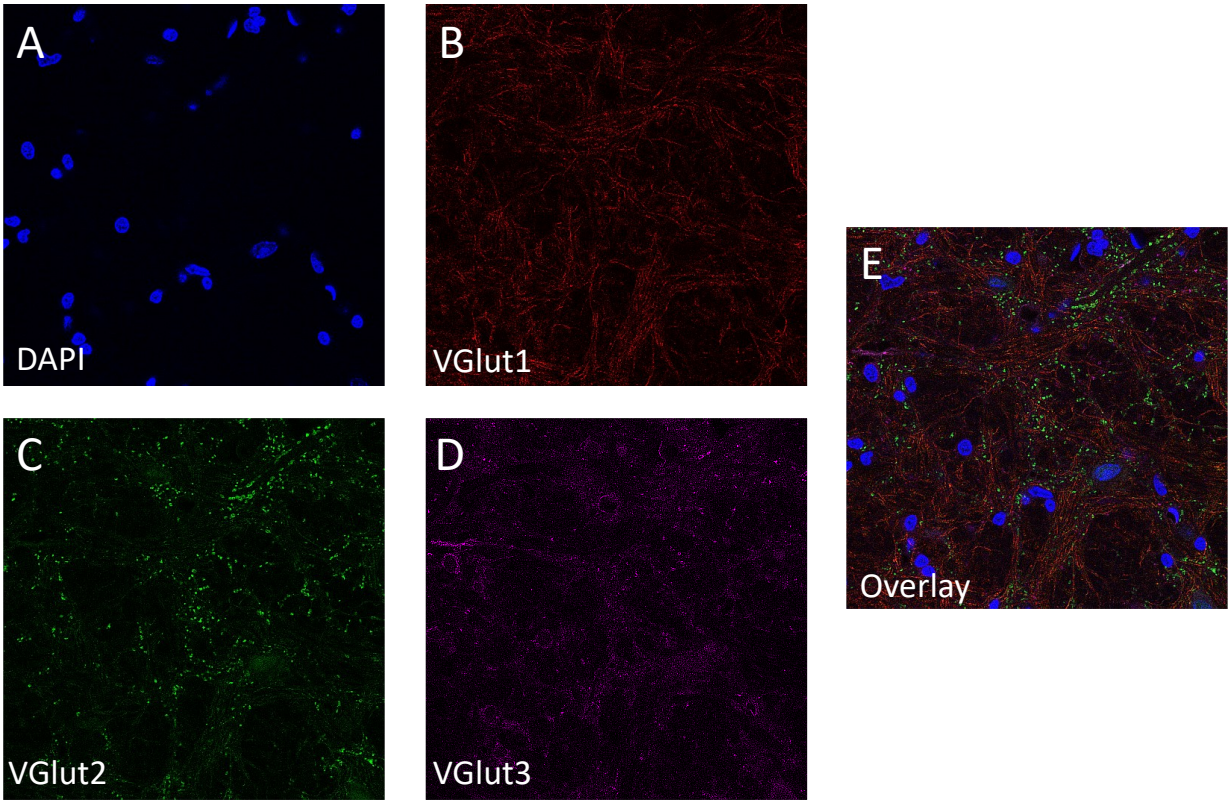

Figure 17 | 40x Magnified Expression of Vesicular Glutamate Transporter 1, 2, and 3 Proteins in the Dorsal Raphe Nuclei Using Sample 3-86.5**.** Sprague-Dawley rat coronal brainstem sections 3-86.5 (harvested a week prior) imaged using a DMi8 confocal microscope at a 40x objective lens with oil immersion (A) Cellular nuclei were stained using DAPI, shown in blue. (B) Vesicular glutamate transporter 1 proteins (VGlut1) were labeled using Alexa 555 secondary antibodies, shown in red. (C) Vesicular glutamate transporter 2 proteins (VGlut2) were labeled using Alexa 488 secondary antibodies, shown in green. (D) Vesicular glutamate transporter 3 proteins (VGlut3) were labeled using Alexa 680 secondary antibodies, shown in purple. (E) Overlay of VGlut1, VGlut2, VGlut3, and cellular nuclei. Sections were 50 um in thickness.

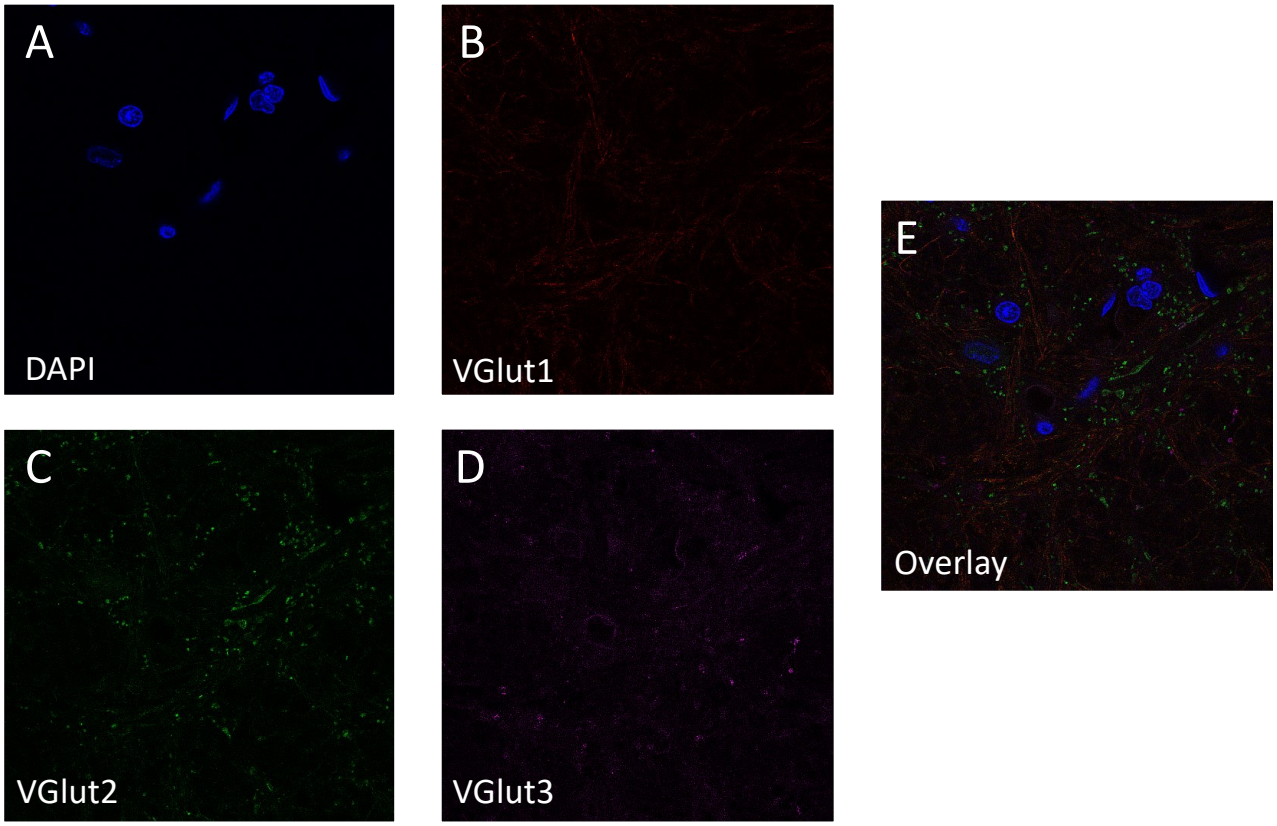

Figure 18 | 63x Magnified Expression of Vesicular Glutamate Transporter 1, 2, and 3 Proteins in the Dorsal Raphe Nuclei Using Sample 3-86.5. Sprague-Dawley rat coronal brainstem sections 3-86.5 (harvested a week prior) imaged using a DMi8 confocal microscope at a 63x objective lens with oil immersion (A) Cellular nuclei were stained using DAPI, shown in blue. (B) Vesicular glutamate transporter 1 proteins (VGlut1) were labeled using Alexa 555 secondary antibodies, shown in red. (C) Vesicular glutamate transporter 2 proteins (VGlut2) were labeled using Alexa 488 secondary antibodies, shown in green. (D) Vesicular glutamate transporter 3 proteins (VGlut3) were labeled using Alexa 680 secondary antibodies, shown in purple. (E) Overlay of VGlut1, VGlut2, VGlut3, and cellular nuclei. Sections were 50 um in thickness.

DISCUSSION

Identification of Dorsal Raphe Nuclei Location via Coronal Brainstem Samples of Saline Treated Rat Models

The first aim of this project was to identify the dorsal raphe nuclei within Sprague Dawley rats via the development of a cresyl violet staining protocol. It was predicted that staining multiple coronal brainstem sections of Sprague-Dawley rats would allow for visualization of core landmark structures around the dorsal raphe nuclei that would indicate the correct stereotaxic location for further study. Tissue samples were first placed on positively charged slides to adhere them prior to staining. During the first trial of cresyl violet staining, tissue samples began to peel off of these positively charged slides as they were submerged within the first three washing solutions. Over 75% of the tissue samples being stained were lost within the solution and became free floating. In attempt to troubleshoot the ability for tissue samples to adhere to the slide surface, four variables were tested: charge of the slides, duration of drying, heat, and method of washing. The charge on the slides were tested by using two types of slides: StarFrost® and Super®Frost Plus slides. Along with two separate slides, each side was tested in the chance that the charge was inadvertently placed on the wrong side. When tissue samples were placed on both slides (and sides) the tissue samples acted in a similar manner and resulted an inability to adhere to the surface of the slides. This concluded that the slides were correctly charged, and the tissue samples were the cause of the inability to adhere.

With the tissue samples unable to adhere to the slides after 12 hours of drying, increased time was given to a max of 48 hours. When the tissue samples were placed on the SuperFrost® Plus slides, KimWipes were used to draw excess PBS from under the samples and off of the

slides before allowing to dry. At the same time, additional tissue samples were heat dried in an oven for 5 minutes and 10 minutes before allowing to sit for 48 hours. It was anticipated that if tissue samples were able to be dried either through heat or longer periods of time then the samples would become adhered to the samples and have a harder time peeling off during the staining process. However, through the course of testing the drying process the tissue became free floating once again in the washing solutions. These results concluded that the tissue samples were not adhering to the slides due to an unknown cause. Multiple samples were tested with the same results. It was hypothesized that the samples were too old, and overly fixed and may have lost some of their capabilities to hold to a charged slide regardless of the drying process.

Unable to submerge the tissue samples in the washing solutions and stain, a new method was developed in order to bypass the need for the samples to be submerged in solution. The cresyl violet protocol was adjusted using a known method in microbiology where staining is done through a drop-wise method. Tissue samples were first stained by free floating in PBS, cresyl violet staining solution, and the dehydrating steps. After staining, tissue samples were placed on the SuperFrost® Plus slides and dried using an oven for 10 minutes. In order to wash the samples without submerging them, slides were placed at a 45° angle and the washing solutions were allowed to pass over the tissue in a dropwise fashion (Figure 6). Upon completion, samples were cover slipped and observed. It was concluded that regardless of the tissues capability to adhere to the surface of the slides, using a drop wise method for the washing of tissues samples would allow for completion of the cresyl violet staining process and the distinct observation of neuronal structures within the coronal brainstem samples.

Although the process was a success, the resulting tissue samples were overstained, and no differentiation of neuronal structures could occur. Thus, an additional washing step was added

after staining with 90% ethanol with acetic acid. Upon completion of the full protocol, tissue samples were stained properly, and neuronal structures were able to be determined.

Coronal brainstem tissue samples were sliced at 30 um using the cryostat and every fifth sample was stained using the cresyl violet protocol. It is known that the dorsal raphe nuclei is located at the stereotaxic coordinates of: anterior-posterior 0.7mm from the lambda, horizontal axis 3.3mm, and lateral 6.4 mm at a 60° angle (Paxinos and Watson, 2007). At this location there are four structural landmarks that can be used to find the notoriously diffuse dorsal raphe nuclei. Observing the tissue samples, the cerebral aqueduct can be seen as an oval opening along the midline of the tissue samples. The cerebral aqueduct is part of the ventricular system within the brain connecting the third ventricle to the fourth ventricle. Within this aqueduct contains cerebral spinal fluid which flows throughout this system and eventually absorbed by granulations, returning the fluid back into venous circulation (Purves et al., 2001). The cerebral aqueduct rests in close proximity to the dorsal portion of the dorsal raphe nuclei subgroups and can be used to locate the correct stereotaxic location of the DRN.

After locating the cerebral aqueduct, the next step is to locate areas in which the dorsal raphe nucleus extends neuronal populations. Of the different areas that receive these projections the superior colliculus can easily be located due to its structure along the posterior midbrain (Figure 6-9). This structure is partially involved in both head and eye motor movements while receiving nerve projections dorsally from the DRN (Janusonis and Foote, 1999). Along with the superior colliculus, the pontine nuclear group located inferior to the cerebral aqueduct can be used to determine the location of the dorsal raphe nuclei. This nuclear group also contains many serotonergic fibers and is the largest of all the precerebellin nuclei. Not only does this nuclear group provide much needed nervous input to the cerebellum but is found along the hindbrain

inferior to the dorsal raphe nuclei (Kratochwil et al., 2017). The last landmark of the dorsal raphe nuclei is the cuneiform nuclear group which also contains many extending fibers associated with the serotonergic system and the pontine nuclear group. The cuneiform nuclear group is located lateral to the pontine nuclear group and inferior to the cerebral aqueduct. Through the use of cresyl violet staining of coronal brainstem sections of Sprangue-Dawley rats, the dorsal raphe nuclei were able to be located and identified utilizing the landmarks associated with the stereotaxic location of the DRN.

Histological Challenges and Outcomes

During the cresyl violet staining step of identifying the dorsal raphe nuclei, tissue samples did not adhere to the positively charged slides consistently. At first, this was attributed to defective slides and subsequent trials lead to the conclusion, this was not the case. After determining the slides to be in good condition, it was thought that the tissue samples could be the cause of lack of adherence to the slides.

4% paraformaldehyde (PFA) is a common fixative for organic tissue samples and is an important step in preservation for histological processing. Paraformaldehyde helps preserve both structural and compositional elements of tissues including proteins and carbohydrates (Thavarajah et al., 2012). The purpose of PFA is to prevent the decomposition and autolysis of the components within tissues. It is PFA and other aldehyde/oxidizing agents that preserve tissues by cross-linking proteins and stabilizing them. Specifically, formaldehyde is one of the smallest aldehydes that is widely used due to its ability to react as an electrophilic molecule and forming many different chemical products. These reactions lead to the formation of the cross

linking of proteins through both intra- and intermolecular interactions (Thavarajah et al., 2012; Kim et al., 2017).

Formaldehyde goes through a multiple step reaction as it begins to change at the molecular level. First, as formaldehyde is introduced to a protein, it begins to react with amino acids and forms covalent bonds. These bonds result in a methylol adduct which is rapidly converted into a Schiff base. These bases along with the methylol adduct as commonly degraded unless a second chemical reaction occurs. If another protein is available in the reaction it will lead to formaldehyde reacting with more amino acids on another molecule and chaining covalent bonds together. This forms what is known as a methylene bridge. As more methylene bridges form within a formaldehyde solution, proteins get increasingly more cross-linked resulting in a stabilized tissue which can be preserved without degrading (Hoffman et al., 2015; Thavarajah et al., 2012).

This pathway occurs when tissues are exposed to different concentrations of formaldehydes and can be altered depending on the concentrations, incubation time, and if there are any other chemicals within the solution. Yet, one reaction stays constant. Formaldehyde reacts with N-terminal amino groups within tissue samples with high affinity to groups such as lysine, histidine and arginine. These groups are typically positively charged. When reactions occur on negatively charged tissues such rat brain tissue used in our experiments, the methylene bridges creating cross-linked proteins tend to become possibly charge due to the affinity of the N-terminal amino groups and formaldehyde (Figure 19) (Hoffman et al., 2015; Thavarajah et al., 2012).

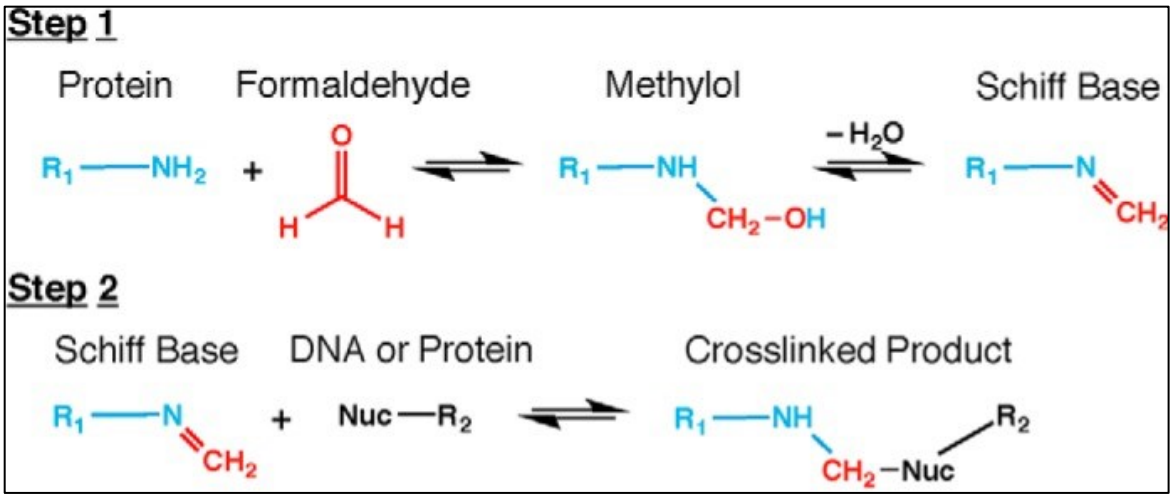

Figure 19 | Chemical Mechanism of Crosslinking Proteins via Formaldehyde. When formaldehyde and a protein interact, they first form a schiff base that can readily react with water to form methylol and vice versa. As more protein interacts with formaldehyde the methylene group binds proteins together via covalent bonds and creates methylene bridges otherwise known as crosslinking of proteins. (Figure taken from Hoffman et al, 2015).

It is thought that tissue samples used in this project did not adhere to the slides due to the fixation process, where tissues were left in 4% paraformaldehyde for approximately 2 years, the cross-linking of proteins caused a change in the net charge of the tissues to positive. Thus, the positively charged slides were not able to hold the positively charged tissues.

In order to overcome this obstacle, the tissue samples were heated inside an oven for a short period of time while on the positivity charged slides. Heat can denature enzymes and proteins which could potentially open up the cross-linked methylene bridges that formed through the fixation process. If the cross-linking covalent bonds were to be broken, the original negative net charge could be restored, and the tissue samples would then adhere to the slides.

Although it was determined that heat treatments were non-affective in adhering the tissues to the slides long term, it did increase the time the tissue samples stayed adhered before peeling off. This indicates that the negative charge could be returning, but due to the length of fixation, they still contained a net positive charge. Thus, the tissue samples were not going to be able to adhere to the slides without possible extensive heat which could damage the samples.

Pulling from past experience in microbiology, one technique used during staining consists of angling the slides and allowing washes to flow over the samples. Although this was used when bacterium was already fixated on slides, it led to trials investigating how we could continue using the tissue samples without complete adhesion to the slides. Tissue samples were stained without adhesion to the slides in order to avoid any issues with the adhesion process. Once stained, the tissues were continued to be exposed to heat in order to break some of the covalent bonds within the cross-linked proteins. With the samples semi-adhered, the slides were angled at a 45 degree and subsequent washes were added to the slides in a dropwise fashion. By

not agitating the tissue samples and using multiple wash flows, the tissue samples were able to stay on the slides and cover slipped.

Visualization of Vesicular Glutamate Transporter Proteins via Immunohistochemistry

A primary objective of this project was the visualization of the vesicular glutamate transporter proteins along the surface of the neuronal cells within the dorsal raphe nuclei. Visualization was addressed by labeling the vesicular glutamate transporter proteins of the dorsal raphe nuclei tissue samples with primary antibodies and their respective secondary antibodies. It was predicted that all three proteins would be able to be visualized within the dorsal raphe nuclei as long as each protein was labeled with different antibodies that fluoresced at distinctly different wavelengths.

Upon successful identification of the dorsal raphe nuclei, immunohistochemistry was conducted to label three distinct transporter proteins in this region. The immunohistochemistry trials began with labeling the vesicular glutamate transporter 2 protein. The first trial contained low concentrations of detergents Triton-X-100 and Tween-20 which led to visualization of glutamate transporter proteins but contained overstaining of the background and non-specific binding which resulted in an inability to differentiate the vesicular glutamate transporter proteins. At this point a third aim was created in order to optimize the IHC protocol to visualize vesicular glutamate transporter proteins without a background signal. Additionally, the optimization would allow reliable reproducibility that could be achieved by an outside individual reducing both cost of animals and chemical reagents.

The concentrations of the detergents were increased in the washing steps of the IHC protocol. Upon completion of the trial with increased concentrations, the vesicular glutamate

transporter 2 protein was successfully labeled with minimal background staining. The successful optimization led to vesicular glutamate transporter 1 and 3 proteins to be labeled alongside the previously labeled transporters. Utilizing the same concentrations of reagents and antibody dilutions, the vesicular glutamate transporter 1, 2, and 3 proteins were successfully labeled with minimal background staining. It was concluded that the protocol was able to be replicated with visualization of three distinct glutamate proteins. The last aim of the project was to analyze the effects of developmental hyperserotonemia on vesicular glutamate transporters within the raphe nuclei. Due to the time constraints and conducting research during a pandemic, this aim was postponed and will be addressed in the future directions.

CONCLUSIONS AND FUTURE DIRECTIONS

ASD presents differently in every individual, varying in severity and symptoms. Additionally, ASD affects the developmental period in individuals to an extent that is not yet fully understood. As such, there is growing interest in studying the relationship of ASD to the neuronal circuitry during development (Jeste, 2011). With high levels of serotonin concentrations bound to platelets being the most consistent biomarker for ASD, it has been proposed that this neurotransmitter could alter neurodevelopmental chemical pathways and effectively alter the serotonergic system and neuronal organization within the central nervous system. It has been reported that irregular serotonin levels do play roles in modulating other neurotransmitters such as glutamate and GABA which could have effects on the reelin system and neuronal outgrowth. These findings have been shown in animal models induced with DHS where exposure to high levels of serotonin developmentally alter behavioral patterns resembling that of ASD. These studies validate the use of the DHS model of Sprague Dawley rats as a model to study ASD in behavioral and neuronal functions, as used in this study.

Through the increase in developmental serotonin, neuronal organization is drastically altered as seen in previous literature. This study originally aimed to assess the changes in neurotransmitter levels and the effect it may have on the migratory pathway of neurons in the central nervous system. It was first established that in DHS models, the dorsal raphe nuclei are a key structure to research as it is an origin in which neuronal fibers migrate throughout the cerebral cortex during development. This study, in part, served to provide preliminary methodological steps to investigate the glutamate transporters within the dorsal raphe nuclei. Along with this, the study aimed to identify the dorsal raphe nuclei through the neuronal

structures found around it. Our findings show that within coronal brainstem sections, the superior colliculus, cuneiform nuclear group, cerebral aqueduct, and pontine nuclear group are all structural landmarks that can be used to identify the DRN.

Further, vesicular glutamate transporter proteins are highly reliant on both the levels of GABA and serotonin during the first stages of development. This study provides evidence that the glutamate neurotransmitter is abundant within the dorsal raphe nuclei and is involved with developmental processes alongside serotonin. Thus, with alternating levels of developmental serotonin, vesicular glutamate transporter proteins may also be alternating, providing an area for further investigation. Utilizing the methods developed and tested from this study, future research could be conducted to investigate the levels of glutamate within the dorsal raphe nuclei when rats are induced with DHS. It is predicted that with high levels of developmental serotonin, receptors will become overloaded and begin to inhibit glutamate output, which would directly affect GABA release. Additionally, if developmental serotonin indirectly affects GABA release, then investigation of reelin release within DRN alongside glutamate would be judicious.

Lastly, throughout this study it has been hypothesized that alternating levels of serotonin and glutamate may be decreasing the release of reelin from Cajal-Retizus cells and disrupting the reelin signaling pathway. The disruption of this pathway could lead to abnormal migration of serotonergic fibers as shown in research conducted by Shehabeldin et al. where lateral migration of neurons was ceased. One such study involving the mature inflamation activation (MIA) model of rats may give rise to future areas of research within ASD.

The creation behind the mature inflammation activation model stems back from research where infection with influenza, rubella virus, herpes simplex virus type 2, and other infections during pregnancy became associated with higher risks of schizophrenia and ASD in offspring. It

was thought that as high levels on pro-inflammatory cytokines such as IFN gamma and interleukins mediated effects of the infection on fetal brains causing altered gene expression, neuronal developmental concerns, and many core characterisicts of schizophrenia and ASD including pre-pulse inhibition, social deficts, motor ambnormalites. It is also known that both schizophrenia and ASD paitents show low levels of reelin during development (Shi et al., 2003; Moreno et al., 2011; Ibi et al., 2020). In 2020, Ibi et al. reported that purified reelin supplimentation was capable of rescueing behavior in MIA model of rats. Therefore, if the MIA model of mice which consistantly express low levels of reelin express schizophrenic and ASD-like behavior but is rescued using purified reelin supplementation, it may be advantageous to test these results in a DHS model of rats. If purified reelin supplementation rescues behavioral changes seen in DHS model of rats, it could lead to further elucidation on if the reelin signaling pathway is indeed disrupted due to a lack of reelin release in both the MIA and DHS models. Overall, there are many avenues for future research in regards to neuronal development and ASD that can further elcuidate our our understading of this complex condition.

REFERENCES

Aaron, E., Montgomery, A., Ren, X., Guter, S., Anderson, G., Carneiro, A.M.D., Jacob, S., Mosconi, M., Pandey, G.N., Cook, E., et al. (2019). Whole Blood Serotonin Levels and Platelet 5-HT2A Binding in Autism Spectrum Disorder. J. Autism Dev. Disord. *49*:2417–2425.

American Psychiatric Association (APA). Diagnostic and statistical manual of mental disorders. 5th ed. Arlington, VA: American Psychiatric Association; (2013).

Azmitia, E.C., and Segal, M. (1978). An autoradiographic analysis of the differential ascending projections of the dorsal and median raphe nuclei in the rat. J. Comp. Neurol. *179*:641–667.

Baio, J. (2018). Prevalence of Autism Spectrum Disorder Among Children Aged 8 Years — Autism and Developmental Disabilities Monitoring Network, 11 Sites, United States, 2014. MMWR Surveill. Summ. *67*.

Baudry, A., Pietri, M., Launay J-M., Kellermann, O., and Schneider, B. (2019). Multifaceted Regulations of the Serotonin Transporter: Impact on Antidepressant Response. Front Neurosci. *13*.

Berger, M., Gray, J.A., and Roth, B.L. (2009). The Expanded Biology of Serotonin. Annu. Rev. Med. *60*:355–366.

Brummelte, S., McGlanaghy, E., Bonnin, A., and Oberlander, T.F. (2017). Developmental changes in serotonin signaling: Implications for early brain function, behavior and adaptation. J. Neurosci. *342*:212–231.

Buchsbaum, I.Y., and Cappello, S. (2019). Neuronal migration in the CNS during development and disease: insights from in vivo and in vitro models. Dev. Camb. Engl. *146*.

Ciranna, L. (2006). Serotonin as a Modulator of Glutamate- and GABA-Mediated Neurotransmission: Implications in Physiological Functions and in Pathology. Curr. Neuropharmacol. *4*:101–114.

Coleman, J.A., Green, E.M., and Gouaux, E. (2016). X-ray structures and mechanism of the human serotonin transporter. Nature *532*:334–339.

Cosgrove, K.E., and Maccaferri, G. (2012). mGlu1α-dependent recruitment of excitatory GABAergic input to neocortical Cajal-Retzius cells. Neuropharmacol. *63*:486–493.

Daws, L.C., and Gould, G.G. (2011). Ontogeny and Regulation of the Serotonin Transporter: Providing Insights into Human Disorders. Pharmacol. Ther. *131*:61–79.

Engel, M., Smidt, M.P., and van Hooft, J.A. (2013). The serotonin 5-HT3 receptor: a novel neurodevelopmental target. Front. Cell Neurosci. *7*:76.

Evers, E. a. T., Sambeth, A., Ramaekers, J.G., Riedel, W.J., and van der Veen, F.M. (2010). The effects of acute tryptophan depletion on brain activation during cognition and emotional processing in healthy volunteers. Curr. Pharm. Des. *16*:1998–2011.

Faras, H., Al Ateeqi, N., and Tidmarsh, L. (2010). Autism spectrum disorders. Ann. Saudi. Med. *30*:295–300.

Frazer, A., and Hensler, J.G. (1999). Serotonin Involvement in Physiological Function and Behavior. Basic Neurochem. Mol. Cell. Med. Asp 6th Ed.

Gaiarsa, J-L., and Porcher, C. (2013). Emerging neurotrophic role of GABAB receptors in neuronal circuit development. Front. Cell Neurosci. *7*.

Galanopoulou, A.S. (2008). GABAA Receptors in Normal Development and Seizures: Friends or Foes? Curr. Neuropharmacol. *6*:1–20.

Garcia, L.P., Witteveen, J.S., Middelman, A., van Hulten J.A., Martens, G.J.M., Homberg, J.R., and Kolk, S.M. (2019). Perturbed Developmental Serotonin Signaling Affects Prefrontal Catecholaminergic Innervation and Cortical Integrity. Mol. Neurobiol. *56*:1405–1420.

Gil, V., Nocentini, S., and del Río, J.A. (2014). Historical first descriptions of Cajal–Retzius cells: from pioneer studies to current knowledge. Front. Neuroanat. *8*.

Hampe, C.S., Mitoma, H., and Manto, M. (2017). GABA and Glutamate: Their Transmitter Role in the CNS and Pancreatic Islets. GABA Glutamate - New Dev. Neurotransmission Res.

Hadjikhani, N. (2010). Serotonin, pregnancy and increased autism prevalence: Is there a link? Med. Hypoth. *74*:880–883.

Hellsberg, E., Ecker, G.F., Stary-Weinzinger, A., and Forrest, L.R. (2019). A structural model of the human serotonin transporter in an outward-occluded state. PLOS ONE *14*:e0217377.

Hoffman, E.A., Frey, B.L., Smith, L.M., and Auble, D.T. (2015). Formaldehyde crosslinking: a tool for the study of chromatin complexes. J. Biol. Chem. *290*:26404-26411.

Hornung, J-P. (2003). The human raphe nuclei and the serotonergic system. J. Chem. Neuroanat. *26*:331–343.

Hornung, J-P. (2010). CHAPTER 1.3 - The Neuronatomy of the Serotonergic System. In: Müller CP, Jacobs BL, editors. Hand. Behav. Neurosci. *21:*51-64.

Hough, L.H., and Segal, S. (2016). Effects of developmental hyperserotonemia on the morphology of rat dentate nuclear neurons. Neuroscience *322*:178–194.

Houwing, D.J., Buwalda, B., van der Zee, E.A., de Boer, S.F., Olivier, J.D.A. (2017). The Serotonin Transporter and Early Life Stress: Translational Perspectives. Front. Cell Neurosci. *11*.

Ibi Daisuke, Nakasai Genki, Koide Nayu, Sawahata Masahito, Kohno Takao, Takaba Rika, Nagai Taku, Hattori Mitsuharu, Nabeshima Toshitaka, Yamada Kiyofumi, and Hiramatsu Masayuki. (2020). Reelin Supplementation Into the Hippocampus Rescues Abnormal Behavior in a Mouse Model of Neurodevelopmental Disorders. Front. Cell. Neurosci. *14*:285.

Janusonis, S., Fite, K.V., and Foote, W. Topographic organization of serotonergic dorsal raphe neurons projecting to the superior colliculus in the Mongolian gerbil (Meriones unguiculatus). (1999). J. Comp. Neurol. *413*:342-55.

Jeste, S.S. (2011). The Neurology of Autism Spectrum Disorders. Curr. Opin. Neurol. *24*:132–139.

Kim, S.H., and Lord, C. (2010). Restricted and Repetitive Behaviors in Toddlers and Preschoolers with Autism Spectrum Disorders Based on the Autism Diagnostic Observation Schedule (ADOS). J. Int. Soc. Autism Res. *3*:162–173.

Kim, S-O., Kim, J., Okajima, T., and Cho, N-J. Mechanical properties of paraformaldehyde-treated individual cells investigated by atomic force microscopy and scanning ion conductance microscopy. (2017). Nano. Convergence *4*:5.

Kratochwil Claudius, F., Maheshwari Upasana, and Rijli Filippo, M. The Long Journey of Pontine Nuclei Neurons: From Rhombic Lip to Cortico-Ponto-Cerebellar Circuitry. (2017). Front. Neural Circ. *11*:33.

Li, Y-W., and Bayliss, D.A. (1998). Presynaptic inhibition by 5-HT1B receptors of glutamatergic synaptic inputs onto serotonergic caudal raphe neurones in rat. J. Physiol. *510*:121–134.

Maenner, M.J. (2020). Prevalence of Autism Spectrum Disorder Among Children Aged 8 Years — Autism and Developmental Disabilities Monitoring Network, 11 Sites, United States, 2016. M.M.W.R. Surveill. Summ. *69*.

Maura, G., Marcoli, M., Tortarolo, M., Andrioli, G.C., and Raiteri, M. (1998). Glutamate release in human cerebral cortex and its modulation by 5-hydroxtryptamine acting at h 5-HT1D receptors. Br. J. Pharmacol. *123*:45–50.

McNamara, I.M., Borella, A.W., Bialowas, L.A., and Whitaker-Azmitia, P.M. (2008). Further studies in the developmental hyperserotonemia model (DHS) of autism: social, behavioral and peptide changes. Brain Res. *1189*:203–214.

Moreno, J.L., Kurita, M., Holloway, T., López, J., Cadagan, R., Martínez-Sobrido, L., García-Sastre, A., and González-Maeso, J. (2011). Maternal influenza viral infection causes schizophrenia-like alterations of 5-HT_2A and $mGlu_2$ receptors in the adult offspring. J. Neurosci. *31*:1863-72.

Paxinos, G., and Watson, C. (2007). The Rat Brain in Stereotaxic Coordinates. New York, USA: Academic Press

Pithadia, A.B., and Jain, S.M. (2009). 5-Hydroxytryptamine Receptor Subtypes and their Modulators with Therapeutic Potentials. J. Clin. Med. Res. *1*:72–80.

Placzek, M., Jessell, T.M., and Dodd, J. (1993). Induction of floor plate differentiation by contact-dependent, homeogenetic signals. Development. *117*:205–218.

Purves, D., Augustine, G.J., and Fitzpatrick, D. (2001). editors. Sunderland (MA): Sinauer Associates

Ranson, S.W., and Clark, S.L. (1959). Anatomy of the Nervous System: Its Development and Function. 10th Revised. W.B. Saunders Company.

Rouhizadeh, M., Prud'hommeaux, E., van Santen, J., and Sproat, R. (2015). Measuring idiosyncratic interests in children with autism. Proc. Conf. Assoc. Comput. Linguist. Meet. *2015*:212–217.

Schain, R.J., and Freedman, D.X. (1961). Studies on 5-hydroxyindole metabolism in autistic and other mentally retarded children. J. Pediatr. *58*:315–320.

Shehabeldin, R., Lutz, D., Karsak, M., Frotscher, M., Krieglstein, K., and Sharaf, A. (2018). Reelin controls the positioning of brainstem serotonergic raphe neurons. PLOS ONE *13*.

Shemer, A.V., Azmitia, E.C., and Whitaker-Azmitia, P.M. (1991). Dose-related effects of prenatal 5-methoxytryptamine (5-MT) on development of serotonin terminal density and behavior. Dev. Brain Res. *59*:59–63.

Shemer, A., Whitaker-Azmitia, P.M., and Azmitia, E.C. (1988). Effects of prenatal 5-methoxytryptamine and parachlorophenylalanine on serotonergic uptake and behavior in the neonatal rat. Pharmacol. Biochem. Behav. *30*:847–851.

Shi, L., Fatemi, S.H., Sidwell, R.W., and Patterson, P.H. (2003). Maternal influenza infection causes marked behavioral and pharmacological changes in the offspring. J. Neurosci. *23*:297-302.

Shih, J.C., Cehn, KJ-S., and Gallaher, T.K. (1995). Molecular Biology of Serotonin Receptors: A Basis for Understanding and Addressing Brain Function. In: Psychopharmacology - The Fourth Generation of Progress. 4th ed. Raven Press.

Siegel, G.J., Agranoff, B., and Albers, R. (1999). Basic Neurochemistry. 6th ed. Lippincott-Raven.

Stahl, S.M. (2015). Modes and nodes explain the mechanism of action of vortioxetine, a multimodal agent (MMA): modifying serotonin's downstream effects on glutamate and GABA (gamma amino butyric acid) release. Spectr. *20*:331–336.

Swenson, R. (2006). Chapter 11: The Cerebral Cortex. Rev Clin Funct Neurosci [accessed 2020 Feb 19]. https://www.dartmouth.edu/~rswenson/NeuroSci/chapter_11.html.

Thavarajah, R., Mudimbaimannar, V.K., Elizabeth, J., Rao, U.K., and Ranganathan, K. (2012). Chemical and physical basics of routine formaldehyde fixation. J. Oral. Maxillofac. Pathol. *16*:400-405.

Whitaker-Azmitia, P.M. (2001). Serotonin and brain development: role in human developmental diseases. Brain Res. Bull. *56*:479–485.

Whitaker-Azmitia, P.M. (2004). Behavioral and cellular consequences of increasing serotonergic activity during brain development: A role in autism? J. Devel. Neurosci. *23*:75–83.

Wu, C., and Sun, D. (2015). GABA receptors in brain development, function, and injury. Metab. Brain Dis. *30*:367–379.

Yan, Z. (2002). Regulation of GABAergic inhibition by serotonin signaling in prefrontal cortex. Mol. Neurobiol. *26*:203–216.

Young, P.A., Young, P.H., and Tolbert, D.L. (2012). Basic Clinical Neuroscience. 2 edition. Lippincott Williams & Wilkins.

Zablotsky, B., Black, L.I., Maenner, M.J., Schieve, L.A., Danielson, M.L., Bitsko, R.H., Blumberg, S.J., Kogan, M.D., and Boyle, C.A. (2019). Prevalence and Trends of Developmental Disabilities among Children in the United States: 2009–2017. Pedi. *144*.

Zaretsky, D.V., Zaretskaia, M.V., Samuels, B.C., Cluxton, L.K., and DiMicco, J.A. (2003). Microinjection of muscimol into raphe pallidus suppresses tachycardia associated with air stress in conscious rats. J. Physiol. *546*:243-50.